U.S.NRC
United States Nuclear Regulatory Commission
Protecting People and the Environment

Technical Letter Report
TLR-RES/DE/REB-2021-13
Enclosure 1

Assessment of Reactor Pressure Vessel Inside Diameter Shallow Surface Breaking Flaws First Progress Report: October 2018

Date:

December 2021

Prepared in response to Task 2 in User Need Request NRR-2017-007, by:

Marvin Smith
NUMARK Associates, Inc.

Terry Dickson
NUMARK Associates, Inc.

Andrew Dyszel
NUMARK Associates, Inc.

NRC Project Manager:

Patrick Raynaud
Senior Materials Engineer
Component Integrity Branch

Division of Engineering
Office of Nuclear Regulatory Research
U.S. Nuclear Regulatory Commission
Washington, DC 20555–0001

DISCLAIMER

This report does not contain or imply legally binding requirements. Nor does this report establish or modify any regulatory guidance or positions of the U.S. Nuclear Regulatory Commission and is not binding on the Commission.

NUMARK ASSOCIATES, INC.

Assessment of Reactor Pressure Vessel Inside Diameter Shallow Surface Breaking Flaws
First Progress Report: October 2018

Prepared For:
U.S. Nuclear Regulatory Commission
Washington, DC

NRC Project Manager and Technical Director:
Patrick Raynaud
NRC/RES/DE/CIB

Prepared by:
Marvin Smith, Terry Dickson, Andrew Dyszel
NUMARK ASSOCIATES INC.

October, 2018

NUMARK ASSOCIATES, INC.

Table of Contents

List of Figures

List of Tables

Acronyms

ASME	American Society of Mechanical Engineers
BWR	Boiling Water Reactor
CPF	Conditional Probability of vessel Failure. The probability is termed conditional because it assumes that the analyzed transient has occurred. To transform CPF into a risk metric it must be multiplied by the probability of the transient occurring.
CPI	Conditional Probability of crack Initiation. The probability is termed conditional because it assumes that the analyzed transient has occurred. To transform CPI into a risk metric it must be multiplied by the probability of the transient occurring.
CTE	Coefficient of Thermal Expansion
EFPY	Effective Full-Power Years
EPFM	Elastic-Plastic Fracture Mechanics
FAVOR	Fracture Analysis of Vessels – Oak Ridge
FEM	Finite-Element Method
ID	Inner Diameter
LEFM	Linear-Elastic Fracture Mechanics
NPP	Nuclear Power Plants
NRC	United States Nuclear Regulatory Commission
ORNL	Oak Ridge National Laboratory
PFM	Probabilistic Fracture Mechanics
PNNL	Pacific Northwest National Laboratory
P-T	Pressure and Temperature Limits
PTS	Pressurized Thermal Shock
PWR	Pressurized Water Reactor
RCS	Reactor Coolant System
RPV	Reactor Pressure Vessel
SFT	Stress-Free Temperature
SIFIC	Stress-intensity Factor Influence Coefficients
TWCF	Through-Wall Cracking Frequency; which is calculated as a product of the CPF and a matrix defining the sequence (or event) frequency of the loading transients. Calculating a mean TWCF for RPVs subjected to pressure and temperature curves (regardless of their origin) requires a statistical representation of the possible transients and their frequencies of occurrence. Compilation of such frequency data for normal operational startup and shutdown transients was not within the work scope of this study; thus, no values of TWCF are reported herein.
WPS	Warm Pre-Stress

1 Introduction

As a follow-up to the 2016 ORNL Report on "The Effect of Shallow Inside-Surface-Breaking Flaws on the Probability of Brittle Fracture of Reactors Subjected to Postulated and Actual Operational Cool-Down Transients: A Status Report" (Reference (1), hereafter referred to as ORNL 2016), additonal literature searches and sensitivity studies have been performed. The Fracture Analysis of Vessels – Oak Ridge (FAVOR - Reference (2)) Version 16.1 Probabilistic Fracture Mechanics (PFM) computer code was used to perform these additional sensitivity analyses to further examine the impact of shallow surface breaking flaws on Reactor Pressure Vessel (RPV) structural integrity. FAVOR PFM analyses were performed to determine whether greater realism with which the flaws, vessel loading history and the cladding are modeled produce any significant change to the results presented in ORNL 2016. As has become standard practice since the Pressurized Thermal Shock (PTS) re-evaluation effort, Warm Pre-Stress (WPS) was applied in the brittle fracture model for these FAVOR analyses.

This progress report describes the results of investigations into the shallow flaw issue, performed from January to October 2018 by NUMARK for NRC.

2 Background

2.1 Objective and Report Outline

The objective of this report is to evaluate shallow surface breaking flaws and determine whether these flaws may impact RPV structural integrity during normal plant cooldown operations.

In Section 3, the effect of cladding thermal-mechanical modeling assumptions on FAVOR predictions are investigated. Specifically, the technical bases for cladding Stress Free Temperature (SFT) are evaluated, and the impact of SFT and cladding thermal expansion coefficient (CTE) on FAVOR results are studied.

In Section 4, the effects of plant cooldown at pressures below the maximum pressure allowed by the ASME Nonmandatory Appendix G to SC-XI procedures are examined. Specifically, both actual and hypothetical cooldowns at lower pressures are analyzed, some idealized transients are described for future analyses, and results are presented for a conservative combination of analysis choices.

Finally, Section 5 examines the potential for WPS effects from prior service history.

2.2 Review of ORNL 2016 Shallow Flaw Evaluation

ORNL 2016 presented FAVOR PFM analyses of surface-breaking flaws that extend through the stainless steel clad into the ferritic steel. Reference (3), *A Generalized Procedure for Generating Flaw-Related Inputs for the FAVOR Code*, Section 8 describes the process to estimate the number of pre-service surface-breaking flaws that penetrate the full thickness of the clad. As shown Figure 9.17 of Reference (3),, the estimated density of flaws that extend 0.03 times the vessel wall thickness (abbreviated as an 0.03 t flaw) is 0.0036589 flaws per square foot. Reference (3) does not show any pre-service surface-breaking flaws deeper than the 0.03 t flaw. However, to better understand the relatively high CPI and CPF for these 0.03 t flaws during a normal cooldown, ORNL 2016 evaluated surface-breaking flaws that extend up to 0.25 times the vessel wall thickness. For consistency, ORNL assumed the same 0.0036589 flaws per square foot density for all surface-breaking flaws. Figure 1, taken from ORNL 2016, defines the surface-breaking flaw geometry, with all flaws circumferentially oriented.

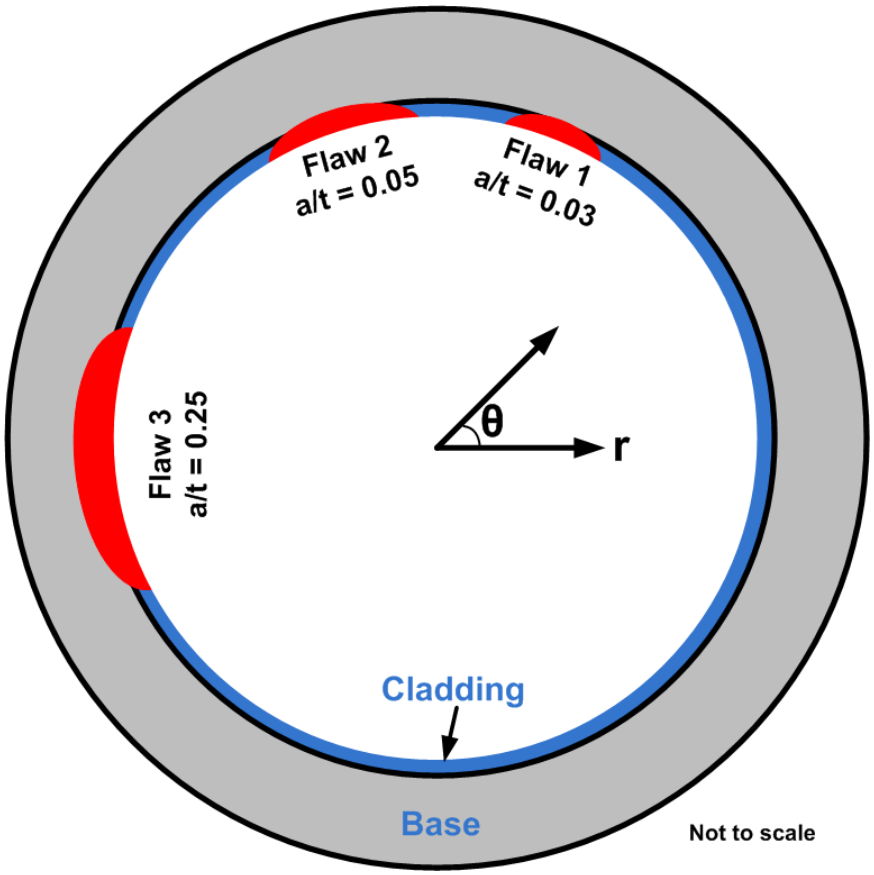

Figure 1: Illustration of Flaw Depth Taken from ORNL 2016 (1)

ORNL 2016 analyzed plant cooldown transients that followed Pressure-Temperature (P-T) curves computed according to ASME Nonmandatory Appendix G to SC-XI (4) using the geometry and neutron fluence associated with the Palisades nuclear power plant RPV at 60 effective-full-power-years (EFPY).[1] ORNL 2016 analyses assumed a constant cool-down rate of 50 °F/hour from reactor operating temperature to ambient. This temperature versus time curve was used with the ASME Nonmandatory Appendix G to SC-XI process to calculate the maximum allowable pressure versus time. ORNL 2016 used this P-T versus time curve (Figure 2) as input to FAVOR PFM analyses to determine the mean CPI as a function of normalized flaw depth for circumferentially-oriented, inner-surface breaking flaws.

[1] Information concerning Palisades was obtained as part of the previous PTS re-evaluation effort. Plant information was used to ensure that typical fleet conditions were studied. However, none of the analyses provided herein provide a replacement for analyses required of the plant.

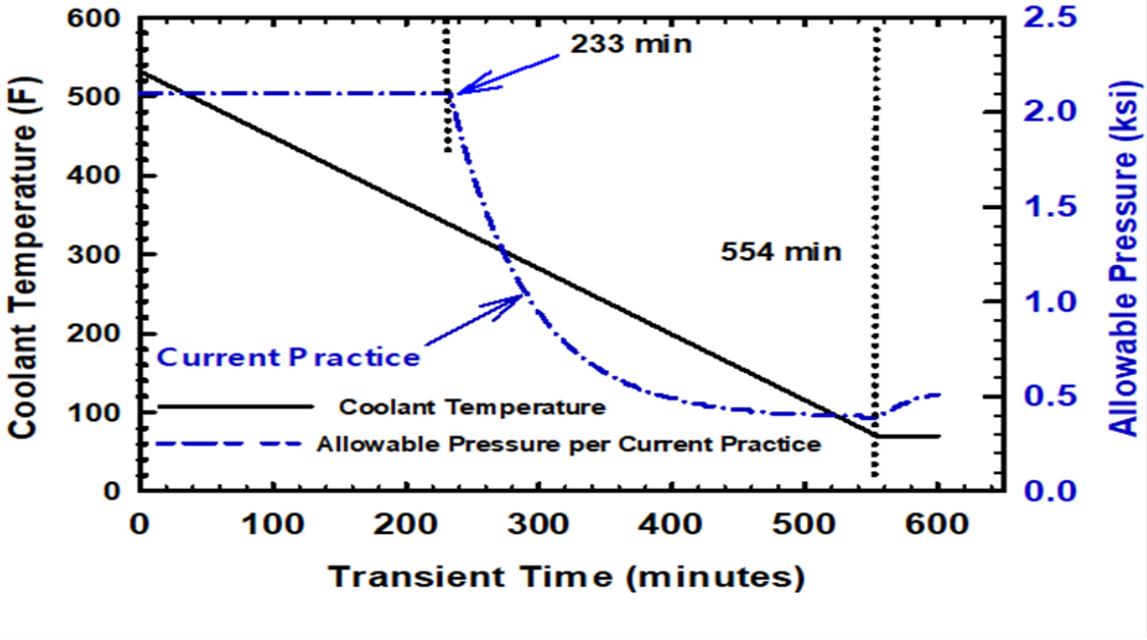

Figure 2: P-T limits for constant 50°F per hour cool-down transient from 532°F to 70°F

The analyses in ORNL 2016 show that flaws that extend just into the ferritic steel have a substantially higher probability of crack initiation (mean CPI) during the plant cooldown scenario shown in Figure 2 than deeper flaws including the 0.25 t flaw used in ASME Nonmandatory Appendix G to SC-XI as a basis for setting the pressure-temperature limits for normal plant heat-up and cooldown operations.

The large drop in CPI shown in Figure 3 for flaws deeper than 0.03 times the vessel wall thickness can be explained by WPS. Figure 4 shows the FAVOR calculated $K_I(t)$ versus time for the 0.03 t and 0.04 t flaws. For the both flaws, there is an initial K_I peak at the transient time (124 minutes) corresponding to the time when pressure is first reduced from the initial 2.1 ksi plant operating pressure. Depending on the flaw depth, the first K_I peak early in the transient may be higher than the second peak. In this example, with WPS, the 0.04 t flaw cannot initiate in cleavage fracture after 124 minutes. At this transient time, the metal temperature and fracture toughness are still relatively high resulting in very low CPI. The maximum value of K_I for the 0.03 t flaw occurs at the time of the second peak, relatively late in the transient, when the metal temperature and fracture toughness are lower resulting in a higher CPI.

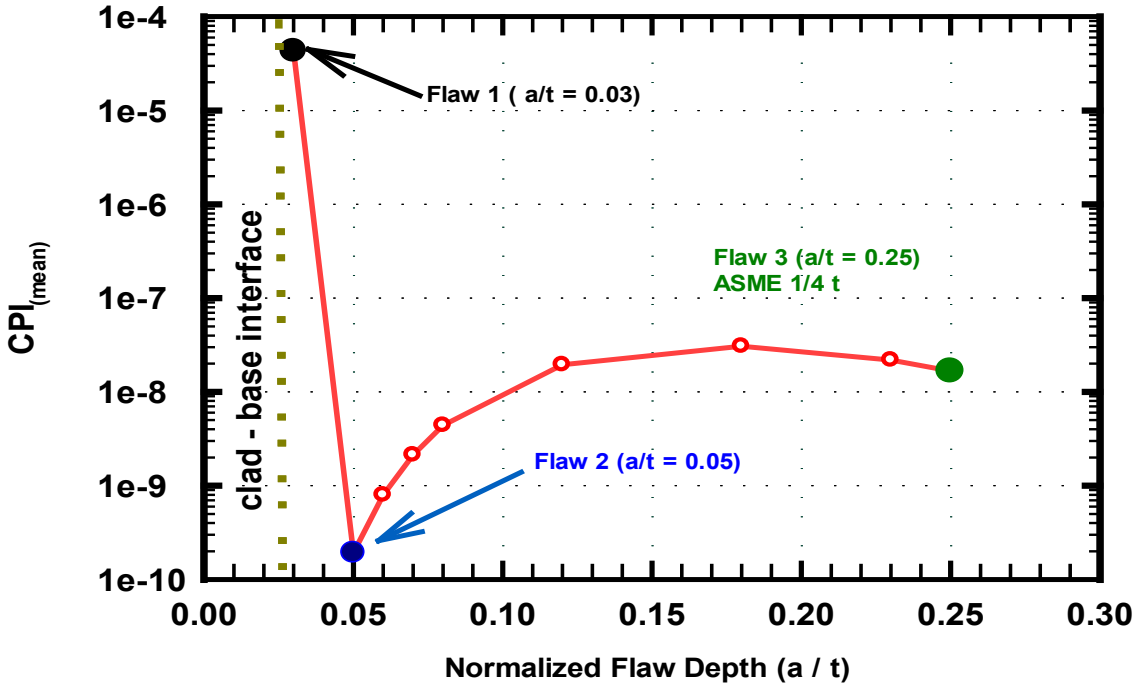

Figure 3: Effect of Flaw Depth on CPI Taken from Figure 1.3 in ORNL 2016 (1)

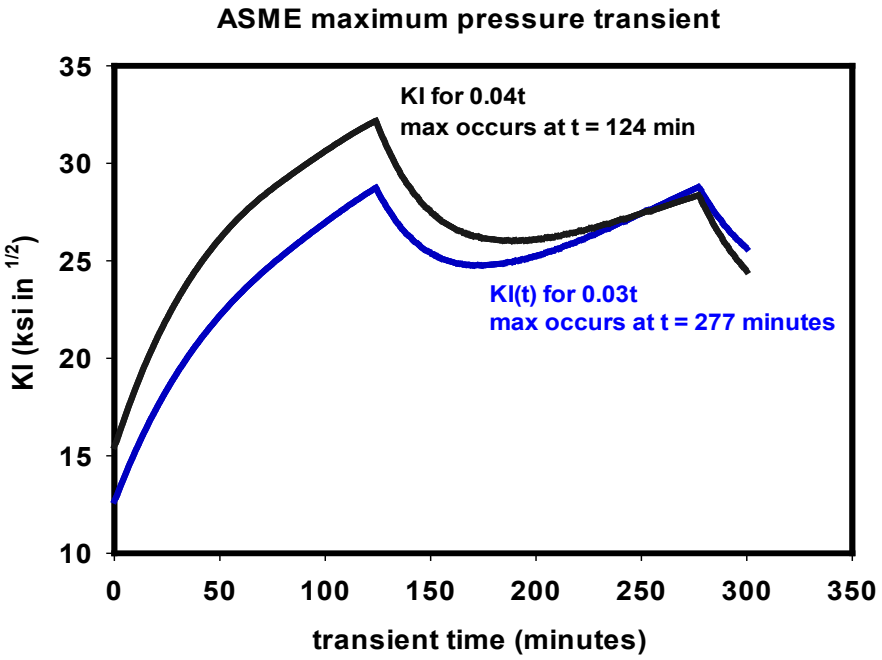

Figure 4: $K_I(t)$ for 0.03 t and 0.04 t Flaws for100°F/hour Cooldown from 532°F to 70°F

2.3 Comparison of FAVOR Version 16.1 with FAVOR Version 15.1

ORNL 2016 shallow flaw analyses were generated by performing PFM analyses with FAVOR version 15.1. FAVOR version 15.1 was a developmental version of FAVOR that was not released publicly. FAVOR version 16.1 (ML16273A033 (2)) is the latest publicly released version of FAVOR. FAVOR version 16.1 K_I solutions for shallow internal surface breaking flaws were verified by comparing FAVOR solutions versus ABAQUS solutions. Appendix G of the 16.1 FAVOR Theory Manual (5) and Reference (2) provide a detailed report of this work.

The same surface-breaking flaw analyses presented in ORNL 2016 were reanalyzed with FAVOR version 16.1 to determine whether there are any significant differences in calculations for mean CPI between FAVOR versions 15.1 and 16.1. FAVOR version 16.1 analyses for the same plant cooldown shown in Figure 2 are compared to the FAVOR version 15.1 analyses as shown in Figure 3. Figure 3 illustrates that mean CPI values calculated with FAVOR version 16.1 are in excellent agreement with the FAVOR version 15.1 ORNL 2016 analyses. Table 1 provides a comparison of the PFM results from FAVOR version 16.1 with the PFM results presented in ORNL 2016. The results nearly identical with just a slight difference in CPI for the deeper flaws. This slight difference may be the result of more RPV trials used in the new FAVOR version 16.1 analyses compared with ORNL 2016 FAVOR 15.1 analyses.

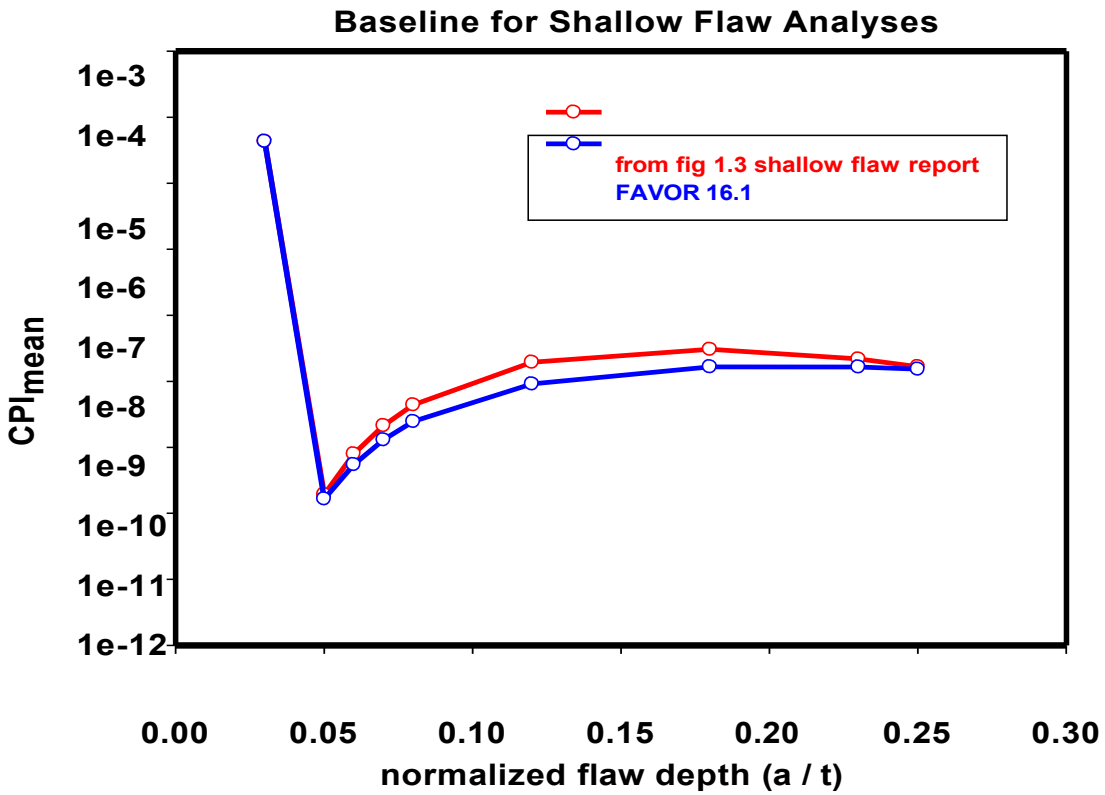

Figure 5: FAVOR Version 16.1 Mean CPI Compared with FAVOR 15.1 Analyses Presented as Figure 1.3 in ORNL 2016

Table 1: PFM Analyses with FAVOR Version 15.1 (Table A5 of ORNL 2016) and FAVOR Version 16.1

Flaw depth (a/t)	ORNL 2016 FAVOR 15.1		FAVOR 16.1	
	CPI mean	CPF mean	CPI mean	CPF mean
0.03	4.33E-05	8.08E-06	4.32E-05	8.93E-06
0.05	1.93E-10	8.36E-14	1.85E-11	4.43E-14
0.08	4.40E-09	1.35E-11	1.95E-09	6.24E-12
0.12	1.95E-08	9.03E-11	1.08E-08	4.42E-11
0.18	3.06E-08	1.89E-10	2.01E-08	6.93E-11
0.23	2.18E-08	6.35E-11	1.61E-08	2.89E-11
0.25	1.67E-08	7.07E-11	1.29E-08	2.80E-11

Based on these comparisons, FAVOR versions 15.1 and 16.1 produce consistent results for the same inputs. Therefore, any differences between this report and ORNL 2016 are the result of differences in inputs and modeling assumptions and are not caused by FAVOR code version differences.

3 Cladding Thermal-Mechanical Modeling

3.1 Discussion of the Technical Basis for Stress-Free Temperature

As discussed in Appendix E of ORNL 2016, FAVOR analyses of K_I use the concept of a Stress-Free Temperature (SFT) to analyze stress resulting from the difference between the Coefficient of Thermal Expansion (CTE) values for the RPV stainless-steel cladding and ferritic steel. ORNL 2016 used an SFT of 488 °F that was developed in a 1999 study from a combination of experimental measurements taken from an RPV shell segment made available from a cancelled PWR and finite element stress analyses using temperature-dependent thermal-elastic material properties. The process used in ORNL 2016 is illustrated in Figure 6. The SFT of 488°F was determined by analysis to produce a tensile stress of 21.3 ksi at 70°F equal to the average measured circumferential CRS as shown in Table 2.

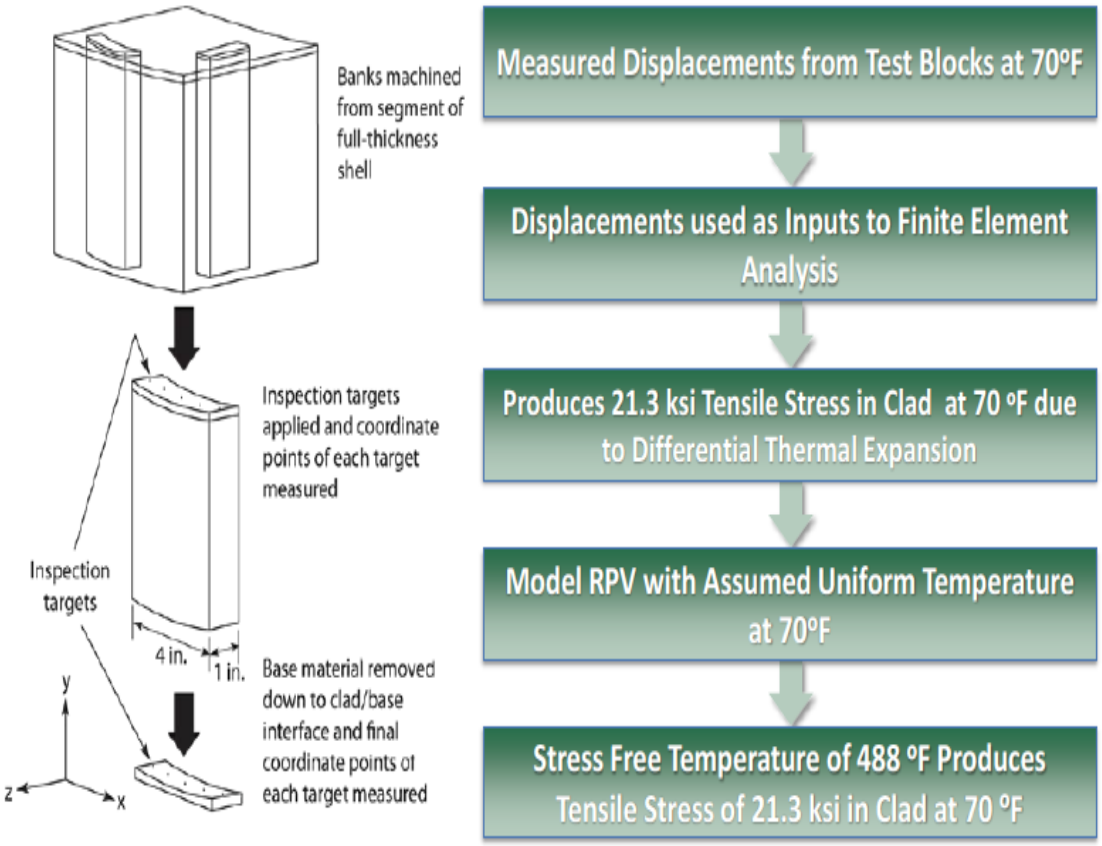

Fig. E-2 Stress-free temperature was determined through combined experimental measurements and finite element analysis.

Figure 6: Process for Determining SFT

Table 2: Table E-2 from Reference (1)

Table E-2 Stress Components Computed from Strains Measured in Cladding taken from a RPV Shell Segment; stresses are calculated at room temperature (70 °F)

Strain Combination	Circumferential Stress (ksi)	Longitudinal Stress (ksi)
Maximum	26.2	17.8
Average	21.3	14.4

As stated in Appendix E of ORNL 2016:
The average value of circumferential stress in Table E-2 was used to calculate SFT; the circumferential and longitudinal stresses would not necessarily go to zero simultaneously, so the calculation was based on the larger circumferential component. That application of FAVOR (utilizing temperature-dependent thermal-elastic material properties) determined that a through-clad, average tensile stress of 21.3 ksi at room temperature of 70 °F corresponds to a value of SFT of 488 °F.

Determination of SFT from combined RPV data/analysis allows FAVOR to account for effects of (1) residual stresses produced by weld deposition of the cladding and (2) mismatch in CTE between the cladding and base metal during any loading transient specified by pressure/temperature versus time curves.

As shown Table 2, the average measured longitudinal stress was significantly less than the measured circumferential stress [14.4 ksi]. Because longitudinal stress is the most important parameter for the shallow flaws that produce the shallow flaw effect, additional ORNL studies were performed after ORNL 2016 was published to determine the SFT for the average longitudinal stress of 14.4 ksi. This evaluation showed that if the temperature of an unloaded vessel is assumed uniform at 70°F then an SFT of 364°F produces an average thru-clad tensile DTE axial stress of 14.4 ksi that exactly offsets the compressive axial stress.

Because a lower SFT would reduce the CPI and CPF for shallow flaws, literature searches and additional evaluations were performed to determine whether (1) there is a firm technical and experimental basis to support a reduction in SFT to a value significantly below 488°F, (2) a case can be developed to support the applicability of any value of SFT in a "one size fits all vessels" manner and (3) whether the use of different SFT values in the axial and circumferential directions violates any solid mechanics rules.

Both SFT values of 488°F and 364°F were developed from a single set of Clad Residual Stress (CRS) measurements of test blocks taken from one RPV. During a literature search for additional CRS measurements, a report published by the Swedish Nuclear Power Inspectorate (SKI), "Cladding Effects

on Structural Integrity of Nuclear Components," Iradj Sattari-Far, Magnus Andersson, June 2006 [Reference (6)] was identified and reviewed.

Section 4 of Reference (6) discusses cladding residual stresses including measurements on:

(1) Reactor vessel head (The Ringhals-2 plant)
   a. The peak of the cladding residual stresses was 400 MPa (58.0 ksi) in the cut-out-piece cladding. This peak showed dropped to 300 MPa (43.5 ksi) and lower in the RPV head cladding. This difference may be explained by relaxation during operation due to service conditions (pressure test, temperature, neutron irradiation).
   b. The stress profile reflects the two-layer nature of the manual weld cladding. For the axial stress component, the behavior does not show a significant difference between the two different locations. However, there is a more pronounced difference for the tangential stress component.

(2) Reactor nozzles (The Lemonitz plant)
   a. Similar results are obtained from the minimum and the maximum clad thickness.
   b. The peak of the cladding residual stresses is between 300 (43.5 ksi) and 350 MPa (50.8 ksi) for this geometry.
   c. The profile of the cladding residual stresses depends on the clad thickness. In the 9 o'clock position, significant tensile stresses exist even in the base material.

(3) Clad plates (Similar to the Oskarshamn-1 RPV)
   a. For measurement of the cladding residual stresses in the test specimens, the hole-drilling techniques and the X-ray diffraction were invoked.
   b. Two major problems in interpretation of the achieved data from the X-ray technique were found. Firstly, the data showed a very large scatter (in some case over 100%). Secondly, the data were not consistent, i.e. they were substantially different in the locations with similar conditions. The measured peak tensile values were about 345 MPa (50.0 ksi) in the center of the plate and about 80 MPa (11.6 ksi) in the center of the cruciform specimen.
   c. The hole-drilling technique was also used for the measurement of the cladding residual stresses, which give information within around 2 mm below the surface.
   d. The measured peak stress was about 200 MPa (29.0 ksi) at 2 mm depth.

(4) Cruciform clad specimens (The NESC-IV project)
   a. Framatome ANP GmbH performed a residual stress measurement using the ring core technique. The measurement was made at the weld on a 100 mm wide strip of a clad beam. The obtained residual stress profiles in different directions are shown in Fig. 4.11 of Reference 2. Here, Direction a is axial, direction b is tangential and direction c is diagonal (45 degrees).
   b. Residual stress in Figure 4.11 peak at a depth of about 4 mm and the peaks stress for directions for a, b and c are similar and the peak is in the range from about 210 MPa (30.5 ksi) to 240 MPa (34.8 ksi).

(5) RPV wall thickness (The ORNL study)

a. Residual stresses from the finite-element analyses for the two cases considered (maximum and average strains) are given to be 148-183 MPa (21.5 to 26.5 ksi) in the circumferential direction and 100-124 (14.5 to 18.0 ksi) in the longitudinal direction.

The CRS measurements reported in Reference (6) range from about 100 MPa (14.5 ksi) to 400 MPA (58.0 ksi). Most of the CRS measurements in Reference (6) are higher than the CRS measurements discussed in ORNL 2016.

Section 4.4 of Reference (6), provides an evaluation of Stress-Free Temperature (SFT) based on a simplified FEM analysis that includes, clad welding, post weld heat treatment, pressure test and plant operation. This Reference (6) analysis estimates a clad SFT of 250°C [482°F] as shown in Table 3 that is close to the SFT of 488°F used in ORNL 2016.

Table 3: Clad Residual Stress [Table 4.4 from Reference (6)]

Table 4.4: Cladding residual stresses at different stages evaluated from FEM analysis.

Loading (point)	Temperature [°C]	Axial stress (σ_{22}) [MPa]	Hoop stress (σ_{33}) [MPa]
After welding (*A*)	20	348	349
PWHT (*B*)	600	-2 [0]	-2 [0]
After PWHT (*C*)	20	135 [241]	136 [242]
Test pressure (*D*)	50	164 [196]	248 [246]
After test pressure (*E*)	20	135 [168]	136 [134]
Operating temperature (*F*)	300	-60 [-137]	-60 [-156]
After operating temperature (*G*)	20	308 [224]	308 [202]
Stress free temperature (*H*)	250 [190]	0 [0]	0 [-20]

*values in brackets are from the simplified analysis.

However, neither the measurements nor analyses in Reference 2 provide a basis for a significant reduction of SFT below 488°F. Therefore, no clear technical basis has been identified to reduce SFT significantly below 488°F.

Several of the CRS measurements in Reference (6) are higher than the CRS measurements used in ORNL 2016 to calculate an SFT of 488°F. The summary of the results of the Reference (6) states that:
The profile and magnitude of the cladding residual stresses depend mainly upon cladding composition, cladding thickness, clad component geometry and temperature. The peak of the cladding residual stresses is about 2-3 mm under the surface of the clad layer, and values in the range of 150 and 500 MPa are reported.

It is reasonable to assume a peak value of cladding residual stresses in the whole clad layer to be equal to the yield strength of the cladding material (around 300 MPa) at room temperature.

Providing that the clad component has received Post Weld Heat Treatment (PWHT), it can be assumed no residual stresses in the underlying base material. For the nuclear pressure vessel, it is also reasonable to assume that the cladding SFT is at the operational temperature of the vessel (around 300°C).

Based on the range of measured CRS and the variety of methods used to apply clad and post weld heat treat the vessel, SFT may be higher or lower than the 488°F used for shallow flaw analyses in ORNL 2016. Therefore. a sensitivity study was performed. as described in Section 3.2to evaluate the sensitivity of shallow flaw CPI and CPF to SFT.

3.2 Sensitivity of CPI and CPF to Clad-Base Stress-Free Temperature

A sensitivity study was performed to determine the sensitivity of shallow flaw CPI and CPF to SFT values from 413°F to 563°F. Three cases were evaluated at SFT values of 413°F, 488°F and 563°F (the recommended 488°F from ORNL 2016 plus and minus 75°F). All three analyses are based on the Palisades embrittlement map at 60 EFPY (same as used in the ORNL 2016 shallow flaw work) and assume a constant cooldown rate of 100°F/hour. The P-T profile followed reduced pressure curve shown in Figure 12.

The FAVOR 0.03 t flaw calculated K_I (Time) for Palisades at 60 EFPY is shown in Figure 7. As shown in this figure, K_I (Time) does not exhibit a first peak because the pressure and temperature are reduced together. For all three SFTs, the peak K_I (Time) occurs at the end of the cooldown. The peak 0.03 t flaw K_I increases from 31.4 to 38.0 (ksi $in^{½}$) as SFT increases from 413 to 563°F. For all three SFT values, the FAVOR calculated 0.03 t flaw K_I (Time) at low temperature exceeds all previous K_I (Time) and the minimum Weibull aK_{Ic} curve. Therefore, the 0.03 t flaw has some potential for crack initiation and vessel failure at all SFT values evaluated. CPI and CPF exceed 1E-06 for all three SFT values. As shown in Table 4, CPI is about 21 times greater for SFT equal to 563°F versus SFT equal to 413°F and CPF is about 38 times greater.

Table 4: CPI and CPF for 413°F, 488°F and 563°F SFT

CPI and CPF for 0.03 t flaw, 'reduced pressure 2' transient (see Figure 12)		
Stress Free Temperature	CPI $_{mean}$	CPF $_{mean}$
413°F	5.99E-05	2.00E-05
488°F	3.28E-04	1.92E-04
563°F	1.25E-03	7.52E-04

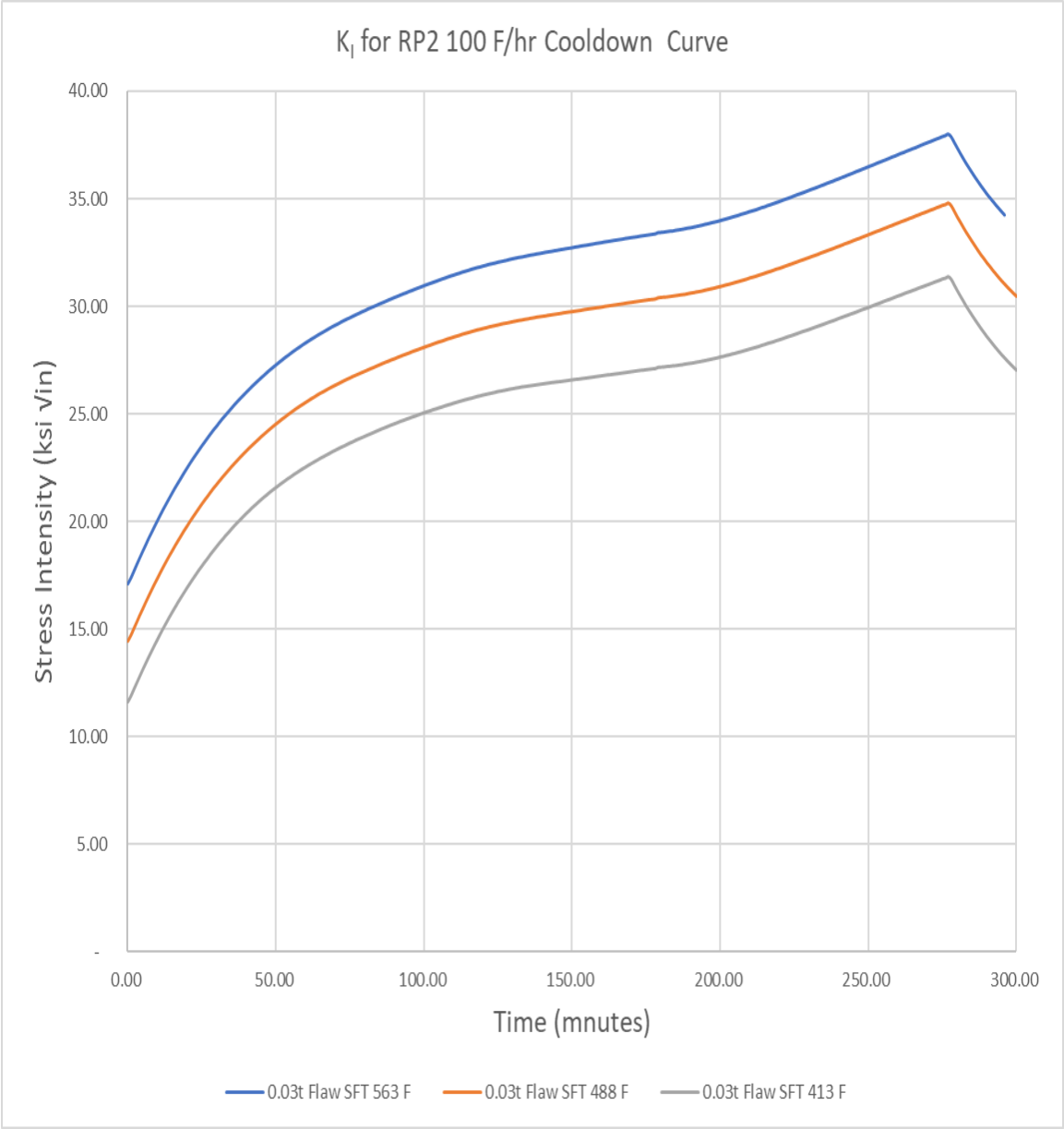

Figure 7: K_I (Time) for 0.03 t Flaw at 413°F, 488°F and 563°F SFT

The FAVOR calculated K_I (Time) for a 0.25 t flaw with 563°F SFT is compared to the K_I (Time) for the 0.03 t flaw in Figure 8. As shown in this figure, the K_I (Time) for the 0.25 t flaw is significantly higher than K_I for the 0.03 t flaw throughout the cooldown. However, the peak K_I for the 0.25 t flaw occurs at a higher temperature. Therefore, crack initiation for the 0.25 t flaw is prevented by WPS.

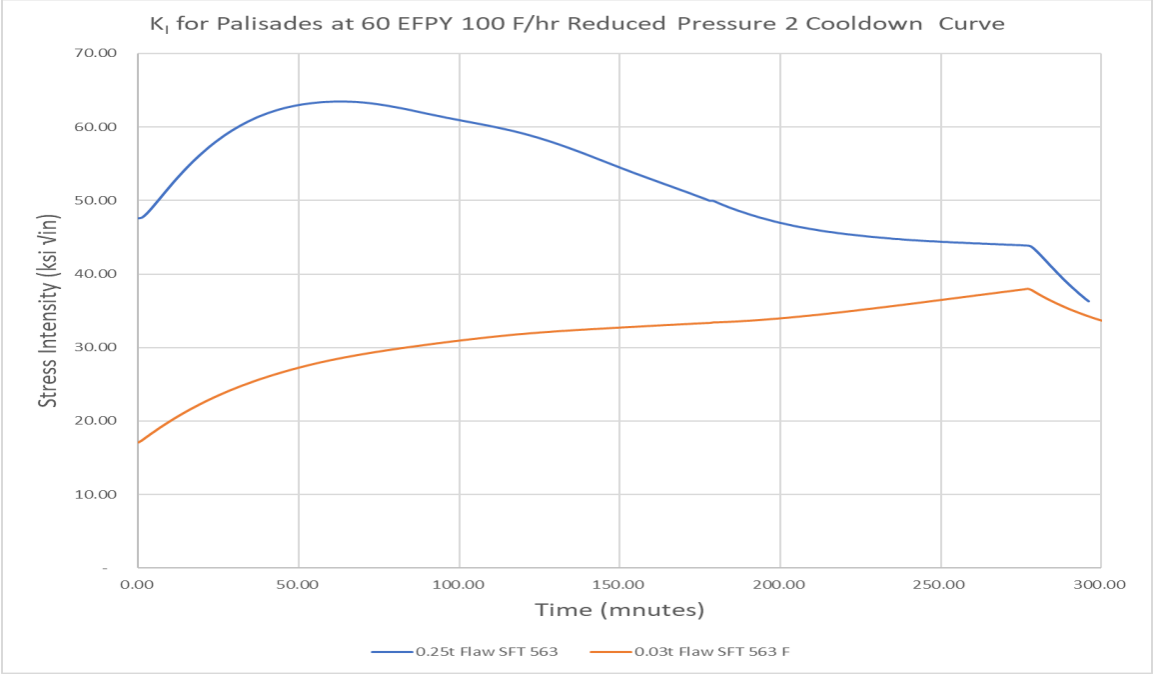

Figure 8: K_I (Time) for 0.03 t and 0.25 t Flaws at 563°F SFT

Based on the literature review of CRS measurements no firm technical and experimental basis was found to support a reduction in SFT below 488°F. Higher CRS measurements than the values used in ORNL 2016 indicate that SFT may be higher than the 488°F used in ORNL 2016. Sensitivity studies of FAVOR calculated CPI and CPF show that the CPI and CPF for 0.03 t flaws may be significantly higher than shown in ORNL 2016 if a higher SFT is used for the FAVOR analyses.

3.3 Sensitivity of CPI and CPF to Clad Coefficient of Thermal Expansion

Section 3.2 of Reference (6) provides a discussion of the clad CTE and provides a formula for estimating stainless-steel CTE. Reference (6) states that "The physical properties of the stainless-steel cladding given by Delfin et al (1998) can be used in conducting thermal analysis of cladding." Reference (6) states that "the thermal expansion of the cladding at different temperature can be obtained from the following equation, NESC-I (2000)."

Equation 1: Reference (6) Equation for Clad CTE

$$\alpha(T) := (15.7 + 0.0096 \cdot T) \cdot \frac{10^{-6}}{\Delta^{\circ}C}$$

The stainless-steel CTE used for FAVOR analyses in ORNL 2016 was taken from ASME Sect. II, Table TE-1, Material Group - 18Cr-8Ni, pages 582-583 (1998). The CTE values from Equation 1 are approximately 4% to 9% higher than the CTE values used in ORNL 2016. During a literature search for CTE, a 2015 ASME reference was identified. This 2015 ASME reference is for austenitic stainless steels (18Cr-8Ni), Material Group 3 and appears on Page 756. As shown in Table 5, the ASME 2015 reference CTE values are approximately 1% to 4% higher than the values used in the ORNL 2016 FAVOR analyses.

Table 5: Stainless Steel Clad CTE

Temp F	FAVOR ASME 1998	ASME (2015)	% difference	SKI Report	% diff
100	0.00000855	0.00000860	0.58%	0.00000892	4.33%
150	0.00000867	0.00000880	1.50%	0.00000907	4.61%
200	0.00000879	0.00000890	1.25%	0.00000922	4.89%
250	0.00000890	0.00000910	2.25%	0.00000937	5.28%
300	0.00000900	0.00000920	2.22%	0.00000952	5.78%
350	0.00000910	0.00000940	3.30%	0.00000966	6.15%
400	0.00000919	0.00000950	3.37%	0.00000966	5.11%
450	0.00000928	0.00000960	3.45%	0.00000981	5.71%
500	0.00000937	0.00000970	3.52%	0.00001011	7.90%
550	0.00000945	0.00000980	3.70%	0.00001026	8.57%
600	0.00000953	0.00000990	3.88%	0.00001041	9.23%

Because differences in CTE between the stainless-steel cladding and the RPV ferritic steel are a potentially important factor in shallow flaw analyses, a sensitivity study was performed to determine the impact of changing clad CTE. Figure 9 shows that the FAVOR calculated 0.03 t flaw K_I (Time) is sensitive to the stainless-steel clad CTE as the temperature approaches 70°F at the end of the cooldown.

In addition to the ASME 1998, ASME 2015 and Reference (6) CTE values, stainless-steel datasheets in Reference (7) [web site for this information is www.atlassteels.com.au] were identified that provide average CTE for several grades of stainless-steel (see Table 6). While these average temperature independent CTE values cannot be readily compared to the ASME and SKI Report temperature dependent CTE values, the range from lowest to highest CTE of 7.9% is similar to the range of CTE values in Table 5.

Table 6: Atlas Steel Reported CTE

SS Type	CTE
316	8.90E-06
302B	9.00E-06
301	9.40E-06
302	9.60E-06
303	9.60E-06
304	9.60E-06

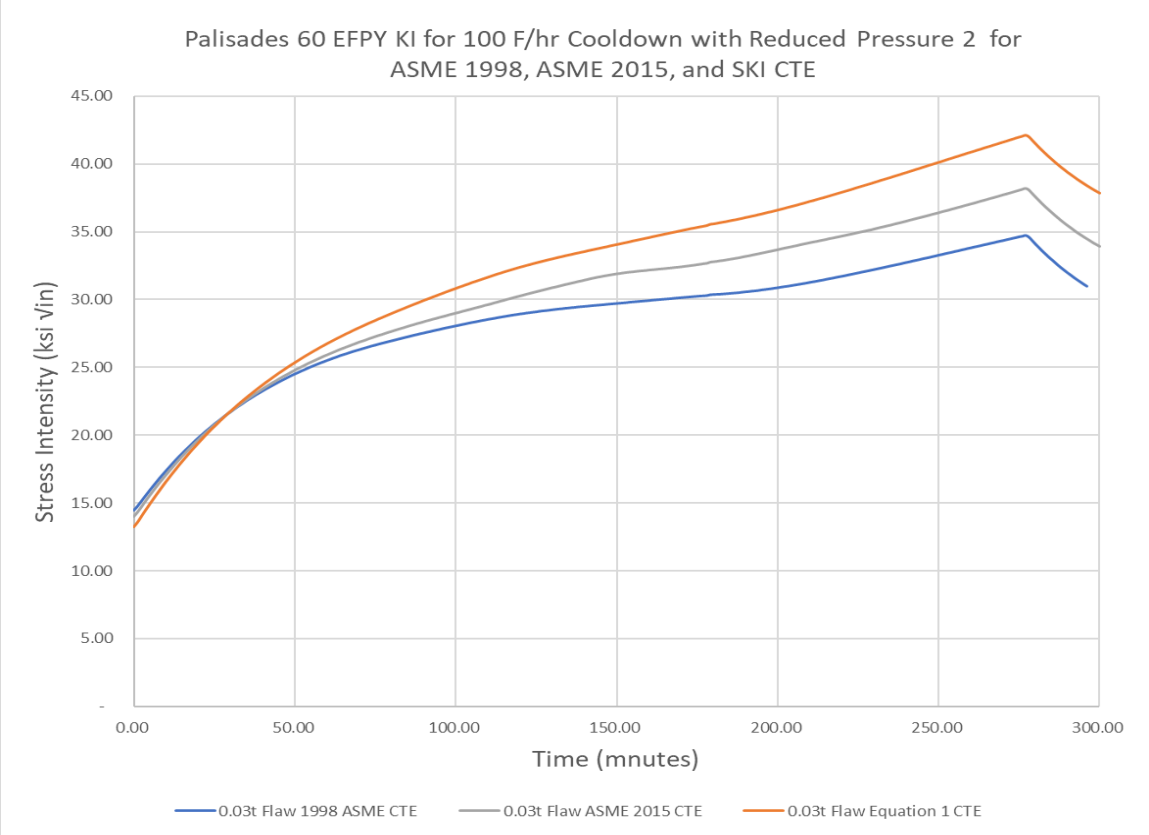

Figure 9: K_I (Time) Comparison for ASME 1998, ASME 2015 and Equation 1 CTE

FAVOR calculated 0.03 t flaw CPI and CPF values are provided in Table 7 for the ASME 1998, ASME 2015 and Equation 1 values of CTE. CPI and CPF are about 3 times higher for the 2015 ASME CTE and about 10 times greater for the Equation 1 CTE compared with the ASME 1998 CTE data used in previous FAVOR analyses. Based on the sensitivity of CPI and CPF to stainless-steel clad CTE and the variability in CTE shown in the literature for different sources and grades of stainless-steel, CTE is an important factor for any shallow flaw analyses.

Table 7: CPI and CPF for 1998 ASME, 2015 ASME and SKI Report Clad CTE

CPI and CPF for 0.03 t flaw, 100°F/hour		
Clad Coefficient Thermal Expansion	CPI_{mean}	CPF_{mean}
ASME 1998 CTE	3.28E-04	1.92E-04
ASME 2015 CTE	1.35E-03	8.40E-04
SKI Clad CTE	4.10E-03	2.28E-03

4 Cooldown Transients

4.1 Impact of Cooldown Pressure Temperature Profile on Surface-Breaking Flaw Analyses

ORNL 2016 analyzed plant cooldown transients using P-T curves computed according to ASME Nonmandatory Appendix G to SC-XI procedures. The analyses in ORNL 2016 maintain the 2.1 ksi plant operating pressure until the maximum pressure calculated according to ASME Nonmandatory Appendix G to SC-XI is less than this normal plant operating pressure. With a cooldown rate of 50°F, full operating pressure of 2.1 ksi is maintained for the first 233 minutes of the cooldown. After 233 minutes, pressure is reduced according the maximum pressure versus temperature allowed by ASME Nonmandatory Appendix G to SC-XI.

With the pressure transient shown in Figure 2, K_I (Time) increases as thermal stress is added to the stress from the 2.1 ksi initial plant operating pressure. With a cooldown rate of 50°F, the maximum pressure allowed ASME Nonmandatory Appendix G to SC-XI drops below the 2.1 ksi initial pressure at 233 minutes into the cooldown. This loading history results in an initial K_I (Time) peak at 233 minutes. As the temperature continues to drop to ambient, the maximum pressure allowed by to ASME Nonmandatory Appendix G to SC-XI levels off at approximately 0.4 KSI and then increases slightly as the temperature approaches ambient. Because the thermal stress continues to increase at lower temperature, there is a second K_I(Time) peak which occurs at the transient time of 277 minutes corresponding to the time when the coolant reaches the assumed ambient temperature of 70°F.

With this loading history, the first K_I peak early in the transient may be higher than the second peak. In this example, with WPS in effect, the 0.04 t flaw cannot initiate in cleavage fracture after 124 minutes. At this transient time, the metal temperature and fracture toughness are still relatively high resulting in a very low CPI. The maximum value of K_I (Time) for the 0.03 t flaw occurs at the time of the second peak, relatively late in the transient, when the metal temperature and fracture toughness are considerably lower resulting in a higher CPI.

The maximum pressure determined according to ASME Nonmandatory Appendix G to SC-XI procedures depends on RT_{NDT}. Figure 10 shows the change in pressure versus time for a 100°F cooldown with an assumed RT_{NDT} of 250°F compared with the Palisades RT_{NDT} of 281°F at 60 EFPY. The maximum pressure allowed by ASME Nonmandatory Appendix G to SC-XI procedures remains above the 2.1 ksi initial pressure for a longer time with the 250°F RT_{NDT} as shown in Figure 10. With this change in pressure-temperature profile, the first peak for the 0.03 t flaw increases to from 34.4 to 35.6 ksi $in^{½}$ whereas the second peak remains the same for both transients at 34.8 ksi $in^{½}$. Therefore, due to WPS, cleavage fracture for the 0.03 t flaw is not possible after the first K_I (Time) peak. The mean CPI for 0.03 t flaw with the RT_{NDT} 281°F pressure versus time shown in Figure 10 is 3.28E-04. This mean CPI for the 0.03 t flaw decreases to 3.05E-8 for the 250°F RT_{NDT} pressure curve. This example illustrates the sensitivity of FAVOR calculated mean CPI to plant loading history.

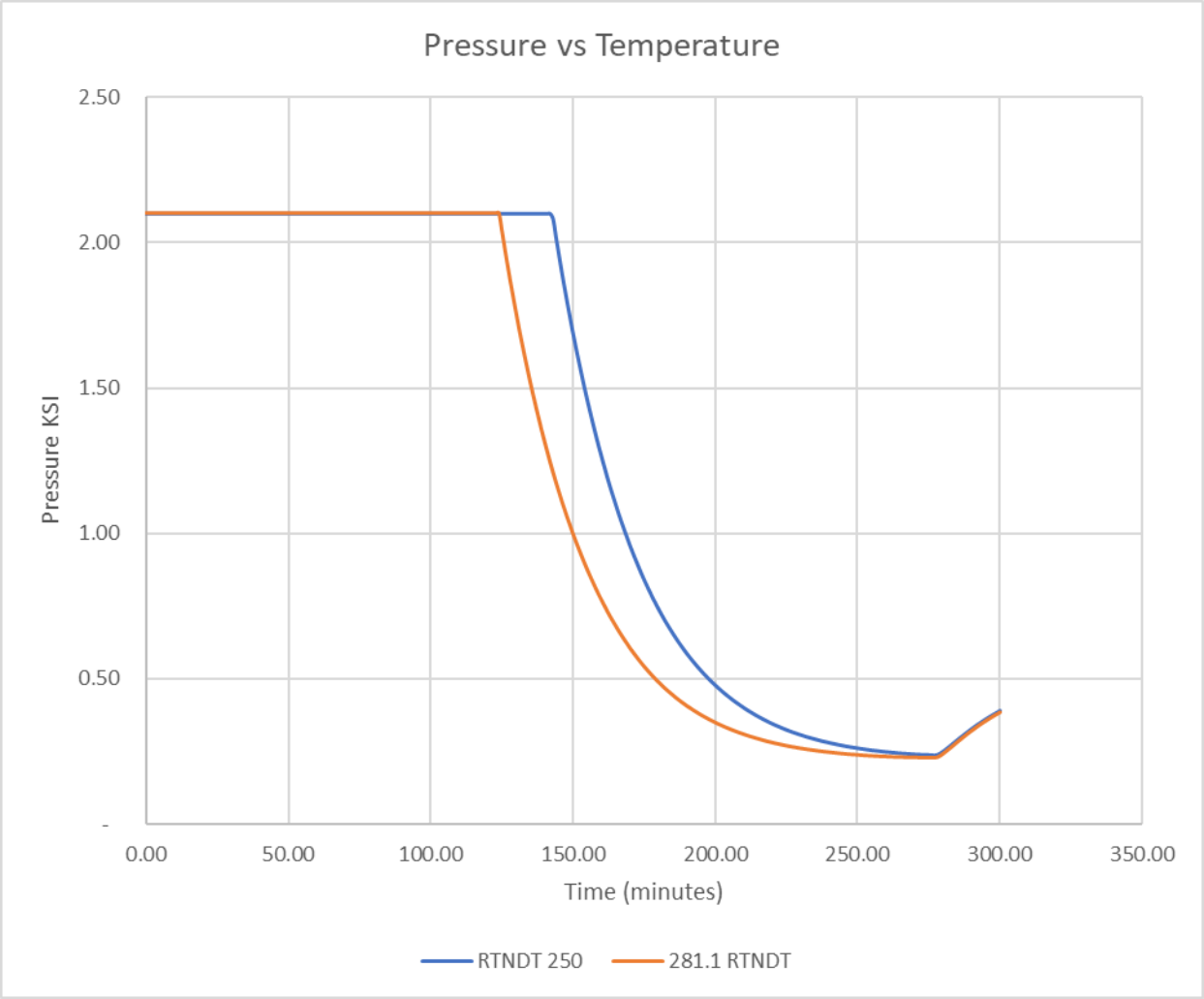

Figure 10: ASME Nonmandatory Appendix G to SC-XI P Maximum Pressure Versus Temperature for RT_{NDT} Values of 250°F and 281.1°F

The stress intensity for a 0.25 t flaw during Palisades normal operation at 2.1 ksi pressure (Figure 11) is 46.7 ksi $in^{½}$. When the 100°F/hour cooldown begins, the 0.25 t flaw K_I (Time) increases to 78.7 ksi $in^{½}$ at the time when the RCS pressure is first reduced below 2.1 ksi. Because the initial K_I (Time) for the 0.25 t flaw is greater the K_I (Time) peak at low temperature, WPS prevents crack initiation for 0.25 t flaws at low temperature for any P-T history. For some shallow flaws, the initial K_I before the cooldown transient begins is less than the final K_I (Time) near ambient temperature. For these shallow flaws, WPS may not prevent crack initiation as the cooldown approaches ambient temperature. Additional cooldowns (see Figure 12) were evaluated to determine whether reducing pressure early in the transient significantly changed mean CPI for shallow flaws.

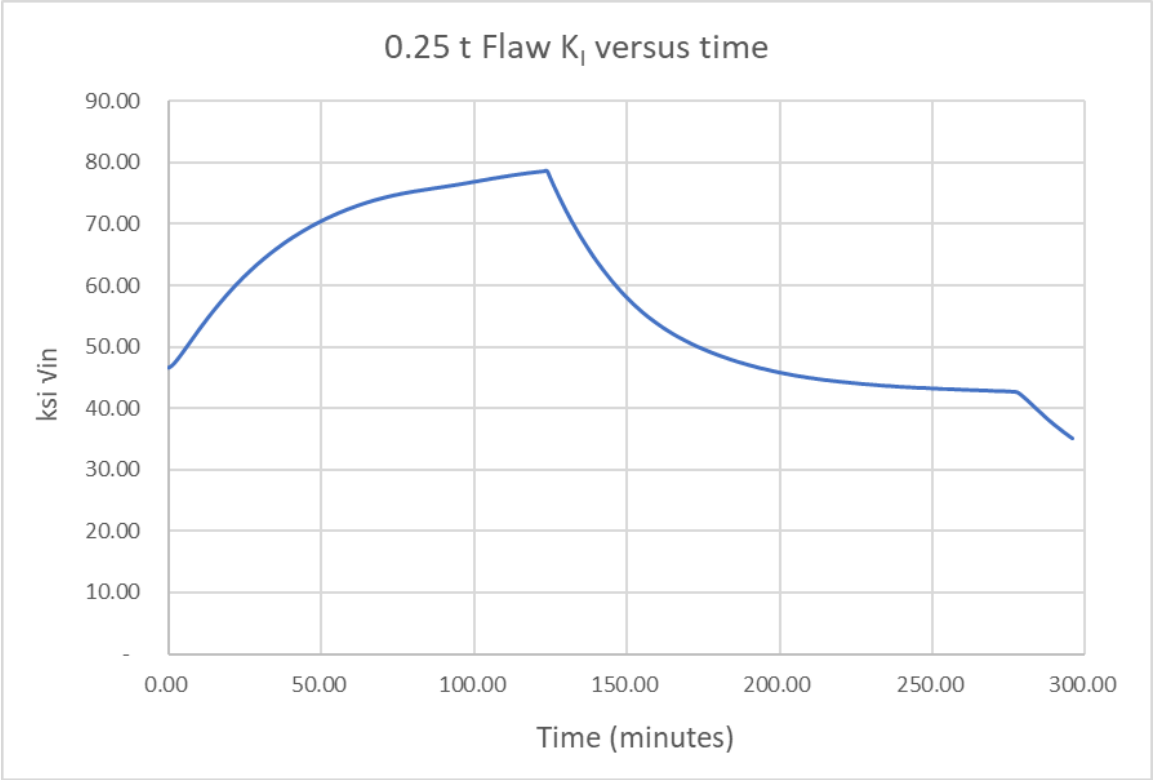

Figure 11: Palisades 0.25 t Flaw K_I (Time) for 100°F Cooldown at ASME Nonmandatory Appendix G to SC-XI Maximum Pressure

Figure 12 shows three potential load histories for a 100°F per hour cooldown from 532°F to 70°F. The transient shown in red maintains the initial operating pressure of 2.1 ksi until the maximum pressure allowed by ASME Nonmandatory Appendix G to SC-XI drops below this 2.1 ksi initial plant operating pressure. From this time until the end of the cooldown, pressure is maintained at the maximum pressure allowed by ASME Nonmandatory Appendix G to SC-XI. The second transient shown in black begins reducing pressure as soon as the cooldown begins. Starting the pressure reduction at the beginning of the cooldown reduces the initial K_I (Time). The black curve is the same as the red curve at lower temperature to maximize pressure stress as the cooldown temperature approaches ambient. The blue curve, labelled near saturation, maintains pressure approximately 0.1 ksi above saturation pressure. At this pressure, WPS early in the transient is minimized and the K_I (Time) is close the minimum value allowed by plant design and cooldown procedures. These loading histories provide a representative range of possible cooldowns allowed by plant design and Technical Specifications.

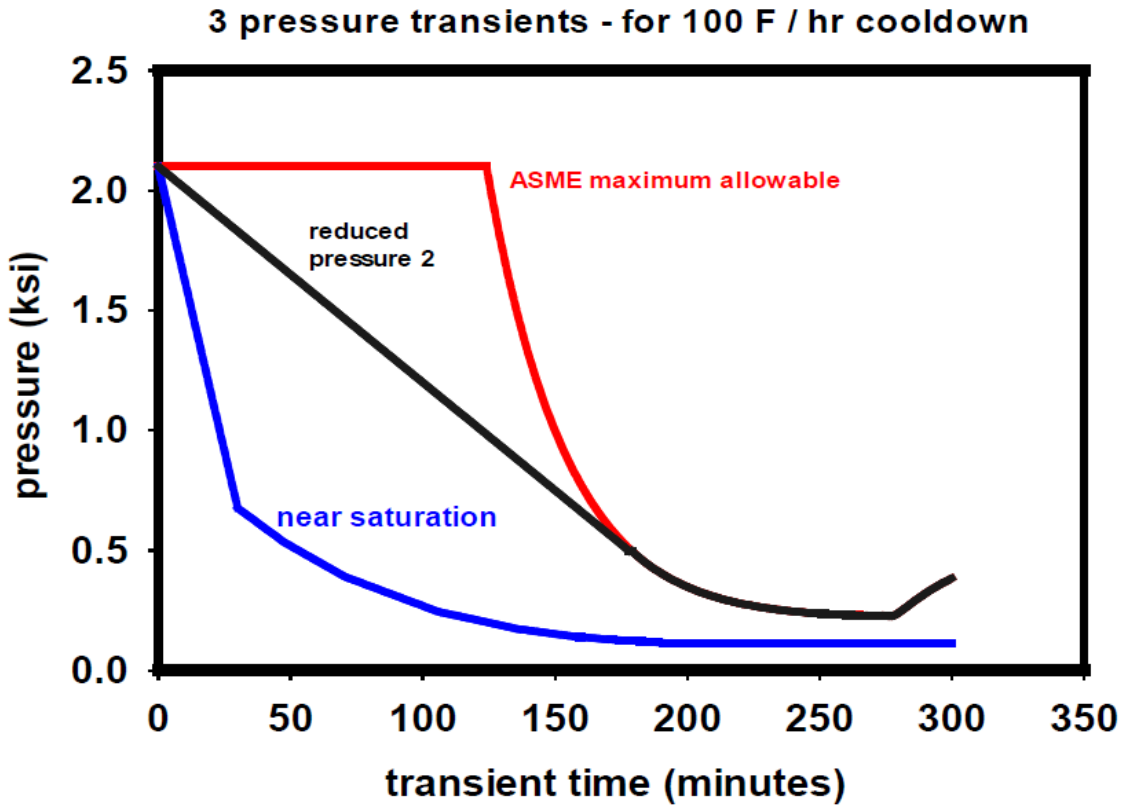

Figure 12: RCS Pressure versus Time for Three Palisades Cooldown Transients

Figure 13 provides FAVOR PFM calculated mean CPI values for surface-breaking flaw depths from 0.03 t to 0.25 t subjected to the three transients illustrated in Figure 12. The FAVOR calculated CPI and CPF values for the flaw depths subjected to the transients in Figure 12 are provided in Table 8. A minimum CPI and CPF of 10^{-9} was assumed for Figure 13 and Table 8 to facilitate plotting on a log scale.

Even though pre-service surface-breaking flaws deeper than 0.03 t are not expected, these analyses assumed the same flaw density for each flaw depth to facilitate comparison of mean CPI for the FAVOR analyses shown in Figure 13 and Table 8. The 0.03 t flaw density generated by the VFLAW computer code was applied to each PFM analyses performed to generate the data points in Figure 13.

As shown in Table 8, the 0.03 t flaw produces the highest FAVOR calculated values for CPI (3.28E-04) and CPF (1.99E-4). The CPI and CPF for the 0.03 t flaw are the same for both the ASME Nonmandatory Appendix G to SC-XI and the reduced pressure 2 cooldown profiles because the pressure near ambient temperature is the same for these two profiles. Reducing pressure early in the transient results in higher CPI and CPF for deeper flaws up to 0.05 t for the reduced pressure 2 profile and for depths up to 0.12 t for the near saturation pressure cooldown. However, the CPI and CPF for these flaws deeper flaws are less than the 0.03 t flaw CPI and CPF. The CPI and CPF for all flaw depths is less for the near saturation pressure cooldown profile because the pressure is lower throughout the cooldown.

These differences in CPI and CPF are explained by the FAVOR WPS model. When WPS is included in the FAVOR analysis, a flaw will not initiate in cleavage fracture unless the K_I (Time) exceeds the value of K_I (Time) at all previous transient times. The K_I (Time) must also exceed the minimum fracture toughness defined by the Weibull lower bound aK_{Ic} (Temperature) distribution used in FAVOR. High K_I (Time) early in a cooldown when the Wiebull lower bound minimum aK_{Ic} (Temperature) fracture toughness is high will not result in cleavage fracture. Additionally, If the K_I (Time) early in a cooldown is greater than the K_I (Time) near ambient temperature, then a flaw will not initiate in cleavage fracture.

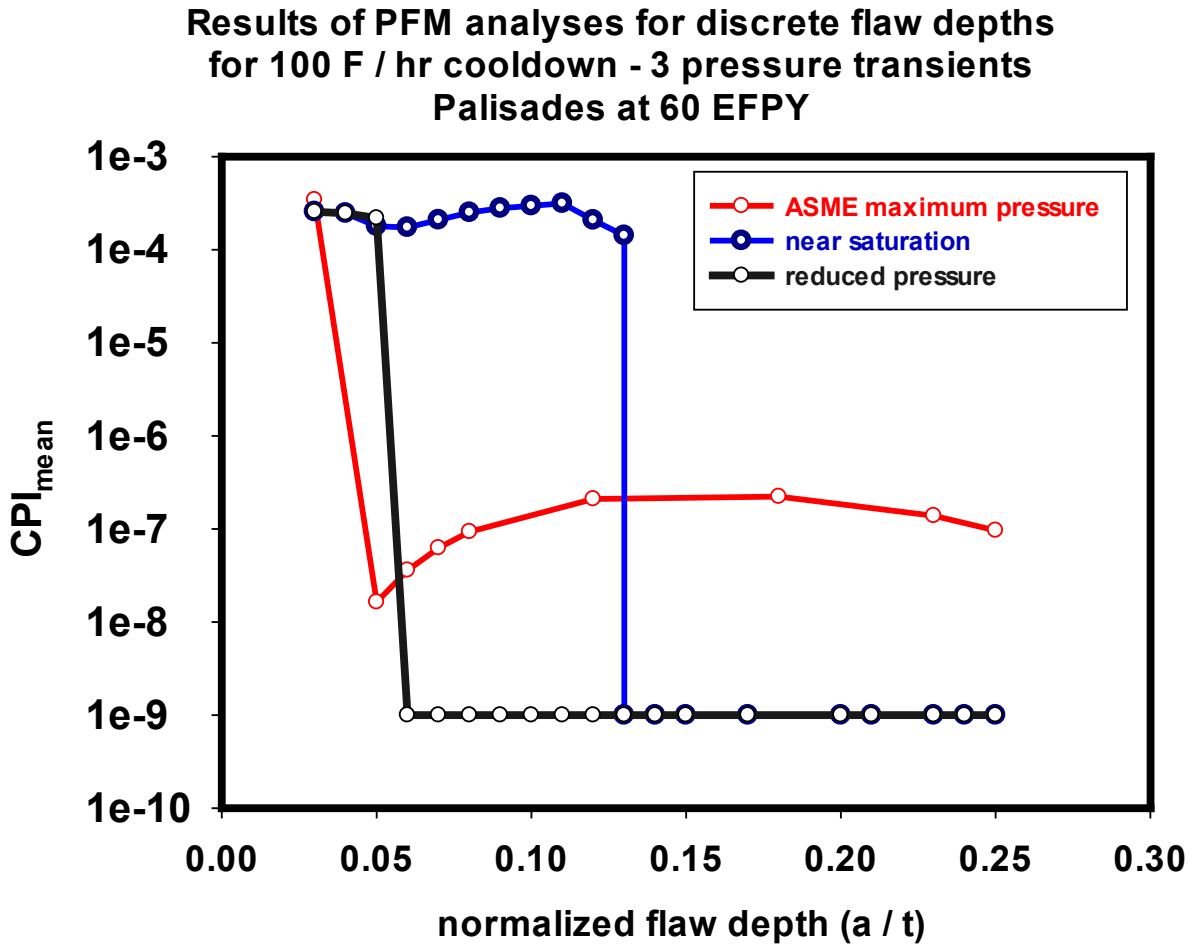

Figure 13: CPI versus Flaw Depth

Table 8: Impact of P-T Curve for Palisades at 60 EFPY with 100°F/Hour Cooldown

Flaw depth	0.1 ksi Above Saturation Pressure		Reduced Pressure 2 Profile		Maximum ASME Pressure RT_{ndt} 281°F	
(a/t)	CPI $_{mean}$	CPF $_{mean}$	CPI $_{mean}$	CPF $_{mean}$	CPI $_{mean}$	CPF $_{mean}$
0.03	**2.54E-04**	**6.88E-05**	**3.28E-04**	**1.92E-04**	**3.28E-04**	**1.99E-04**
0.04	**2.46E-04**	**4.75E-05**	**3.24E-04**	**1.64E-04**	1.00E-08	1.00E-09
0.05	**1.78E-04**	**3.46E-05**	**2.19E-04**	**1.10E-04**	1.62E-08	1.00E-09
0.08	**2.51E-04**	**2.90E-05**	1.00E-09	1.00E-09	9.28E-08	1.45E-09
0.12	**2.07E-04**	**1.89E-05**	1.00E-09	1.00E-09	2.08E-07	2.73E-09
0.18	1.00E-09	1.00E-09	1.00E-09	1.00E-09	2.21E-07	2.61E-09
0.23	1.00E-09	1.00E-09	1.00E-09	1.00E-09	1.33E-07	1.00E-09
0.25	1.00E-09	1.00E-09	1.00E-09	1.00E-09	9.58E-08	1.00E-09

Note: bold value represent CPF higher than 1E-06, which was the threshold for further investigation

4.2 Evaluation of Actual Plant Cooldown Transients

The four actual plant transients shown in the ORNL 2016 are evaluated here to compare with the cooldown at a constant rate of 100°F/hour from 532°F to 70°F. Cooldown at a constant rate of 100°F/hour to ambient is allowed by plant Technical Specifications but does not represent a typical cooldown. Actual plant cooldowns are generally slower than 100°F/ hour and may not cooldown to ambient, especially if the cooldown is not associated with a refueling outage that requires removal of the reactor vessel head.

The first actual cooldown evaluated (Transient 1) involved a cooldown over approximately 14 days as shown in Figure 14. The pressure in Transient 1 remained close to system pressure for the first five days and above 0.3 ksi for remainder of the transient. Based on this pressure history, Transient 1 probably occurred during an outage for plant repair work that was not involved with a refueling. Transient 1 is an example of a cooldown where the pressure remains close to full system operating pressure for an extended time.

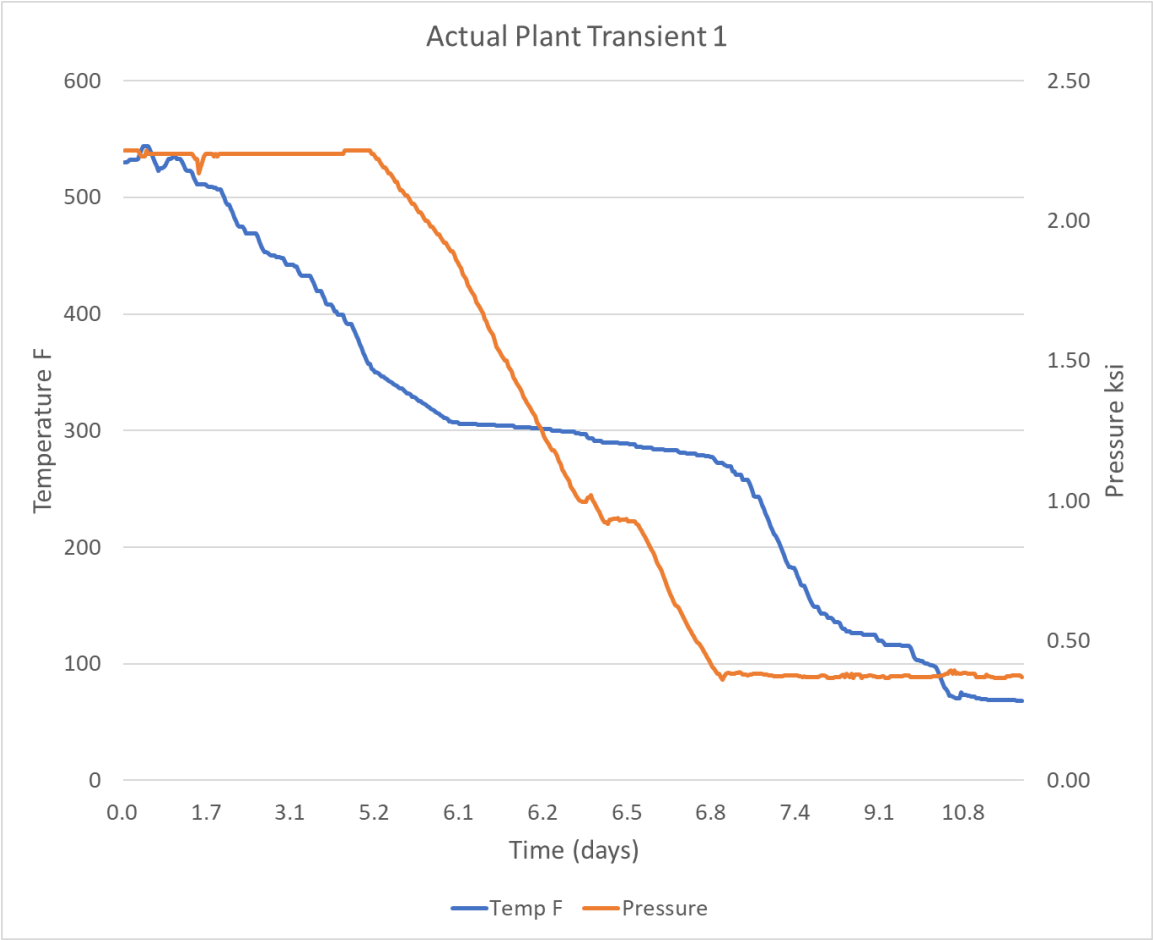

Figure 14: Plant Transient 1 Pressure and Temperature versus Time

Transient 1 was analyzed with FAVOR for the 0.03 t flaw and the K_I (Time) for this transient is shown in Figure 15 along with a plot of the lower bound Weibull aK_{IC} curve. The 0.03 t flaw has an initial K_I (Time) peak approximately 6 days into Transient 1. There is a second higher peak K_I (Time) peak at about 10 days when the Reactor Coolant System (RCS) temperature drops below 100°F. Because this second K_I (Time) peak is higher than any previous K_I (Time) and higher than the lower bound of the Weibull curve, there is some probability of crack initiation.

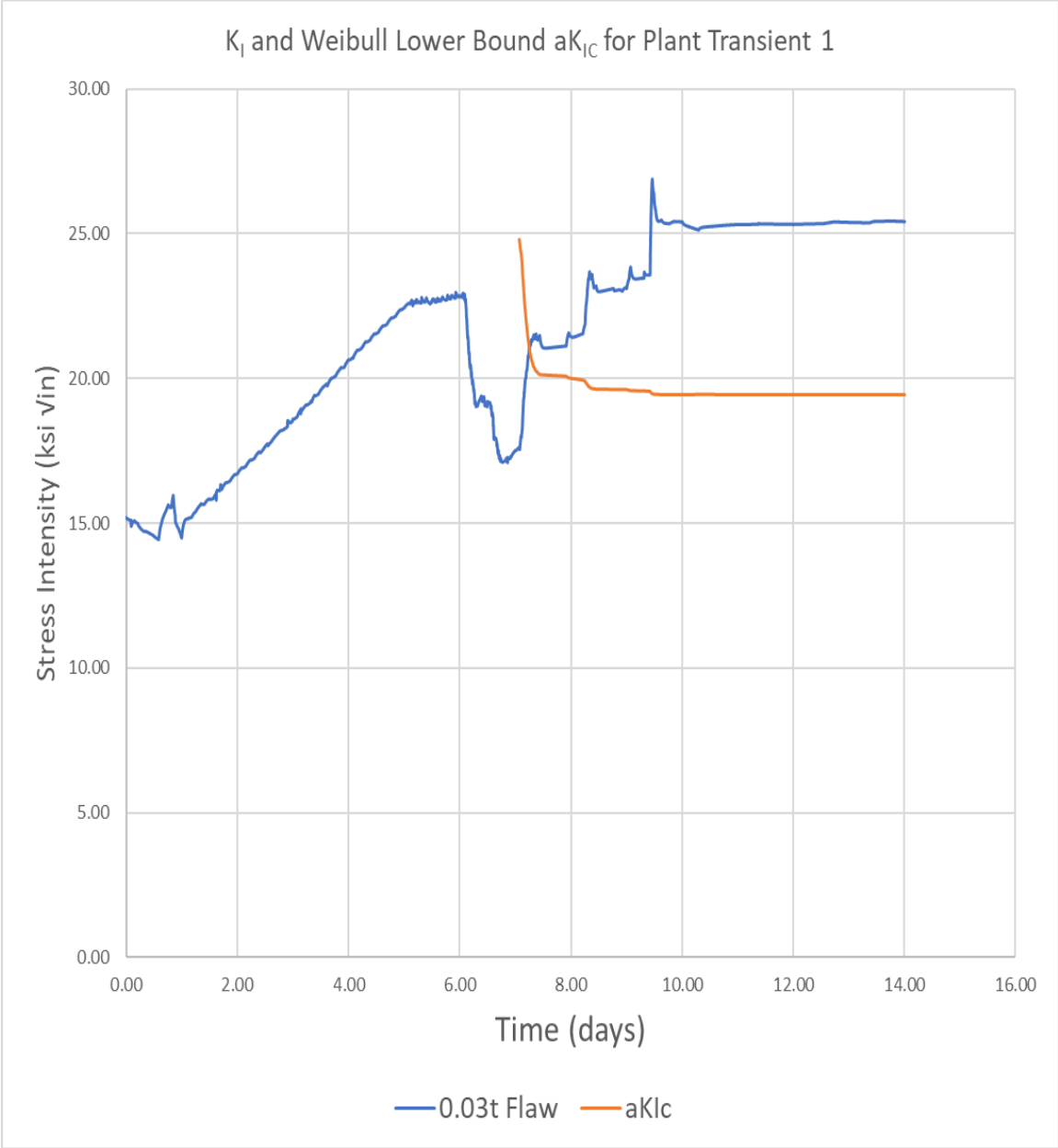

Figure 15: K_I versus Time for Transient 1

Transient 2 involved a cooldown over approximately one day from hot zero power to cold shutdown including a reduction in pressure consistent with removal of the reactor vessel head to allow for a refueling outage as shown in Figure 16. In actual plant Transient 2, the plant operator appears to have reduced both temperature and pressure together to support removal of the reactor vessel head for a refueling outage.

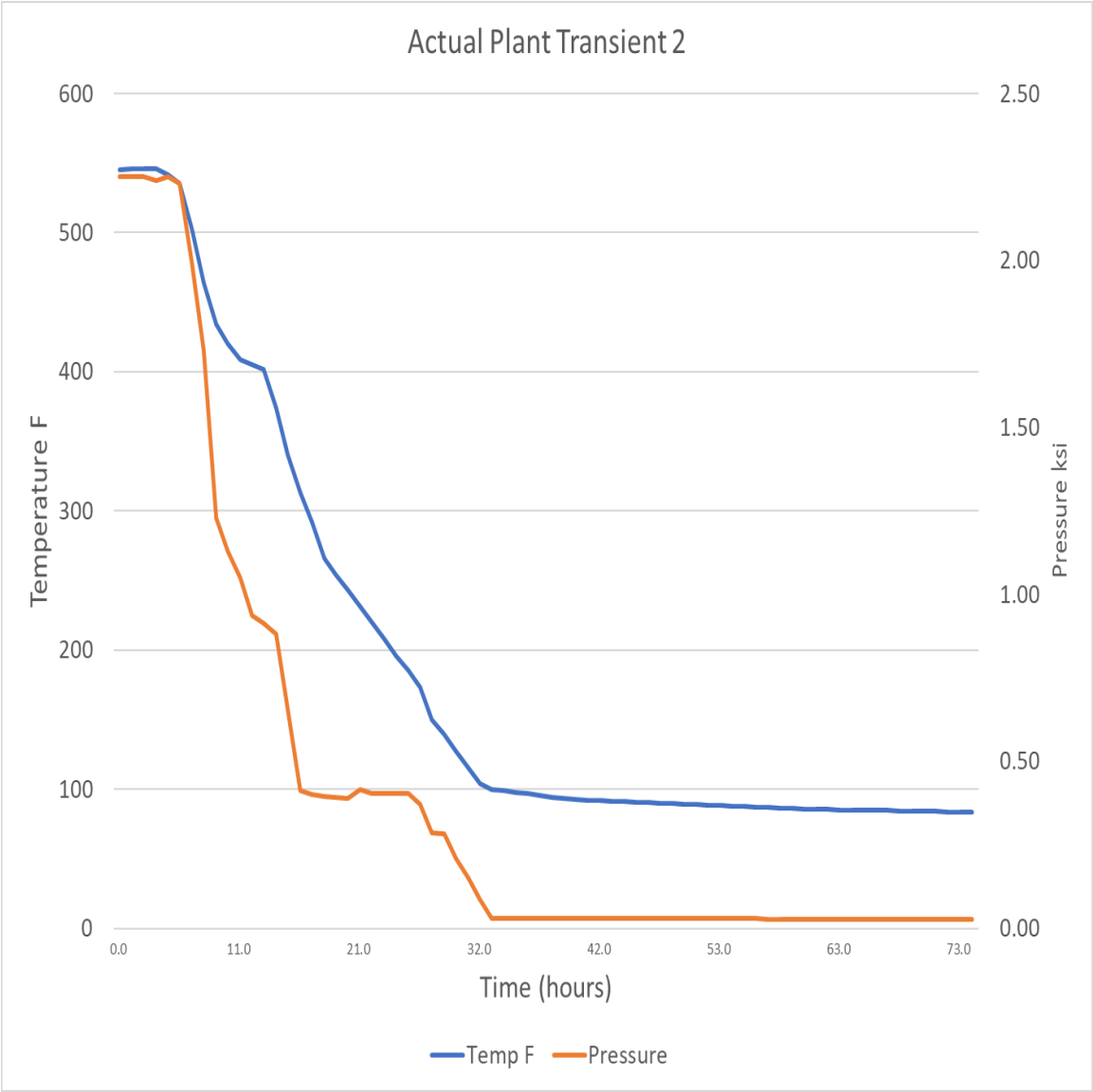

Figure 16: Plant Transient 2 Temperature and Pressure versus Time

Transient 2 was analyzed with FAVOR for 0.03 t flaw and the K_I (Time) for this transient is shown in Figure 17 along with a plot of the lower bound Weibull aK_{IC} curve. The 0.03 t flaw has an initial K_I (Time) peak approximately 6 hours into Transient 2. There is a second higher peak K_I (Time) peak at about 32 hours when the RCS temperature drops below 100°F. Because this second K_I (Time) peak is higher than

any previous K_I (Time) and higher than the lower bound of the Weibull curve, there is some probability of crack initiation.

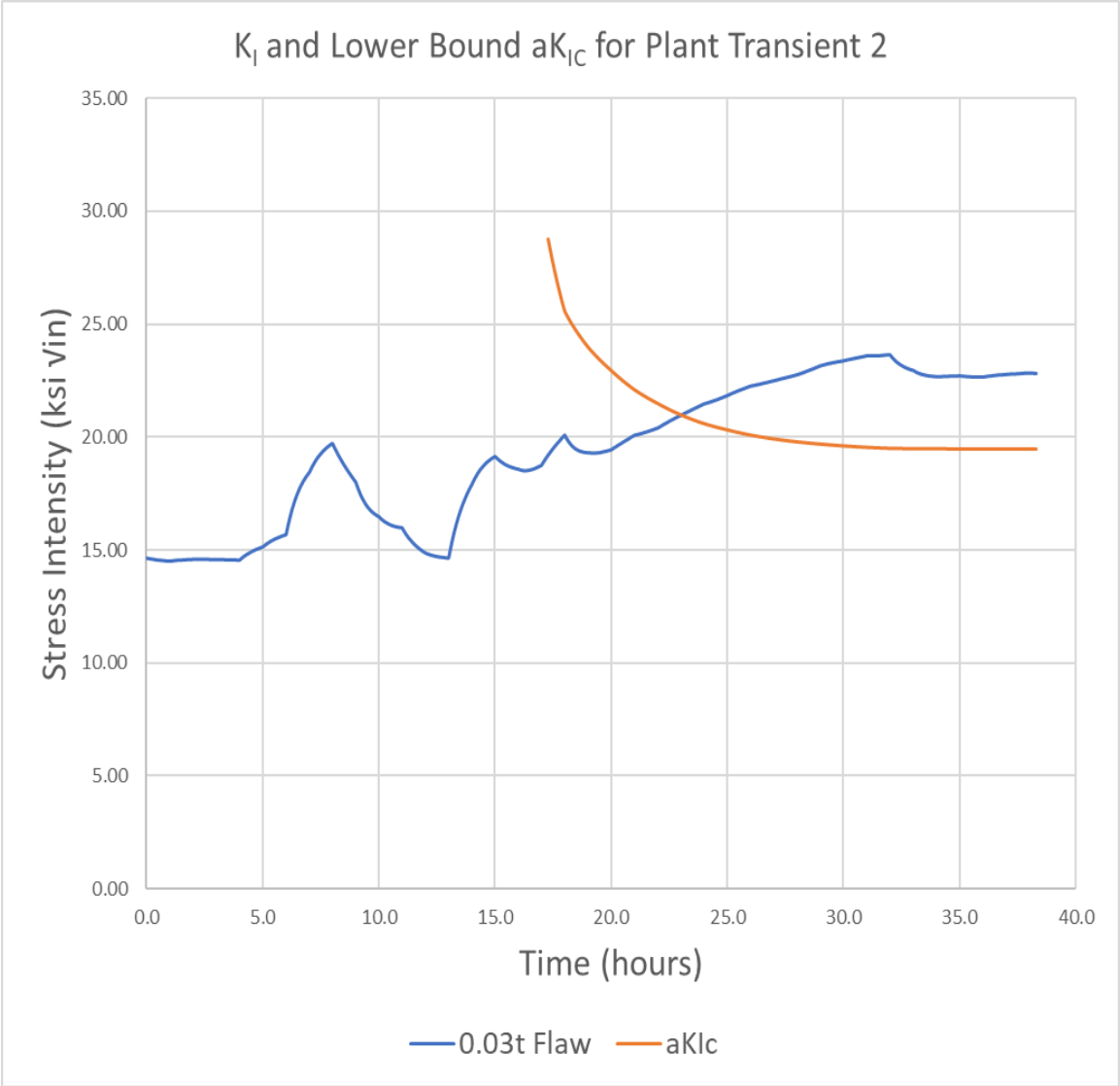

Figure 17: K_I versus Time for Transient 2

Plant Transient 3 involved an initial cooldown to about 320°F over one day followed by about six days at this temperature and then about twenty days of slow temperature reduction as shown in Figure 18. During Transient 3, the system pressure was first reduced to about 0.9 ksi, then increased back to about 1.7 ksi before finally being reduced to about 0.25 ksi. Based on the pressure versus time for Transient 3, this transient was probably the result of an equipment failure or other issue that required an extended time to correct.

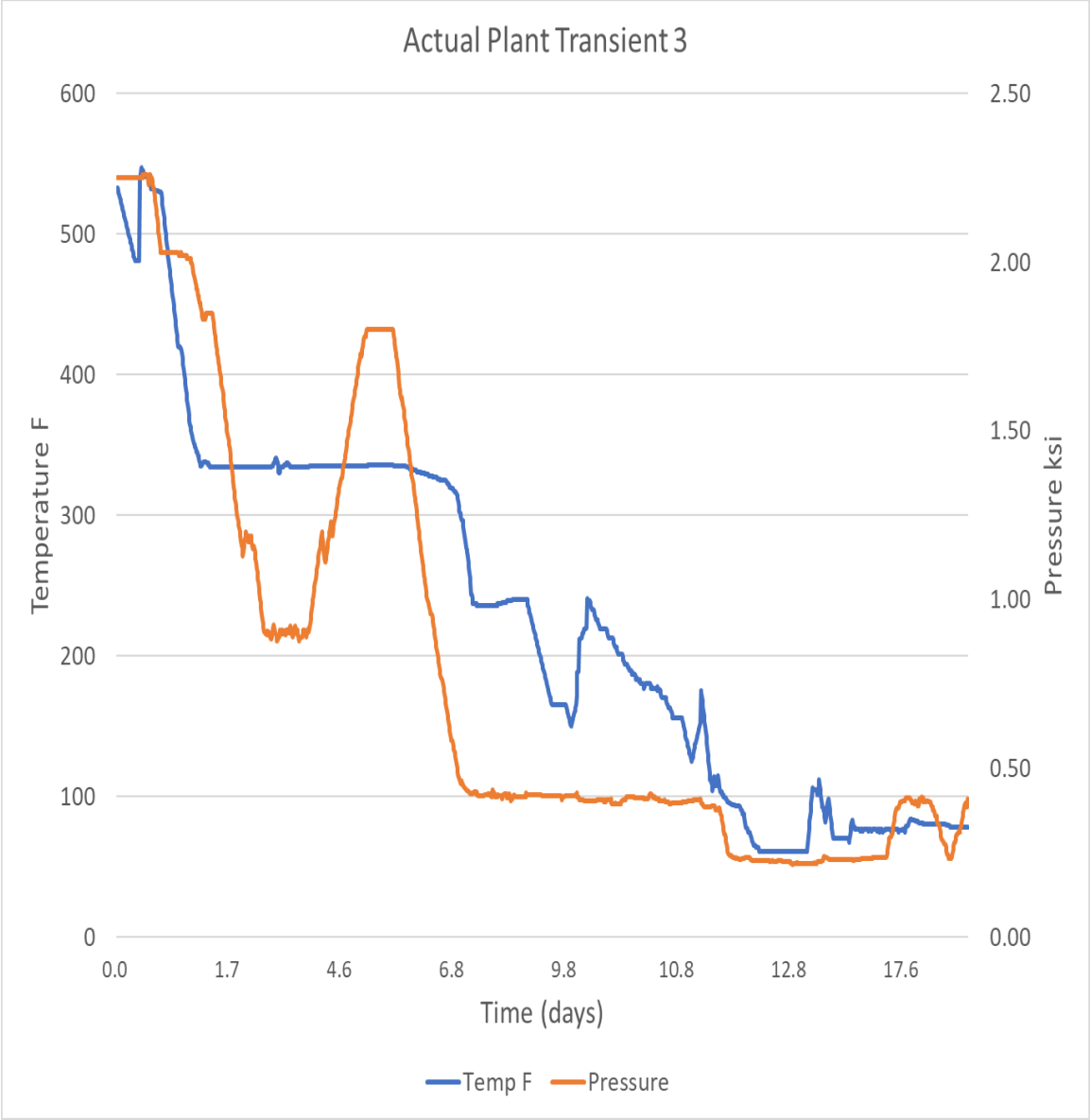

Figure 18: Plant Transient 3 Temperature and Pressure versus Time

Because Plant Transient 3 included several times when pressure and temperature both increased and decreased, the K_I (Time) for Transient 3 exhibits a complicated pattern as a function of time. Transient 3 was analyzed with FAVOR for 0.03 t flaw and the K_I (Time) for this transient is shown in Figure 19 along with a plot of the lower bound Weibull aK_{IC} curve. The 0.03 t flaw has several K_I (Time) peaks. The K_I (Time) peak just before 10 days into the transient when the RCS temperature drops below 100°F is the highest K_I (Time) for this transient. Because this K_I (Time) peak is higher than any previous K_I (Time) and higher than the lower bound of the Weibull curve, there is some probability of crack initiation.

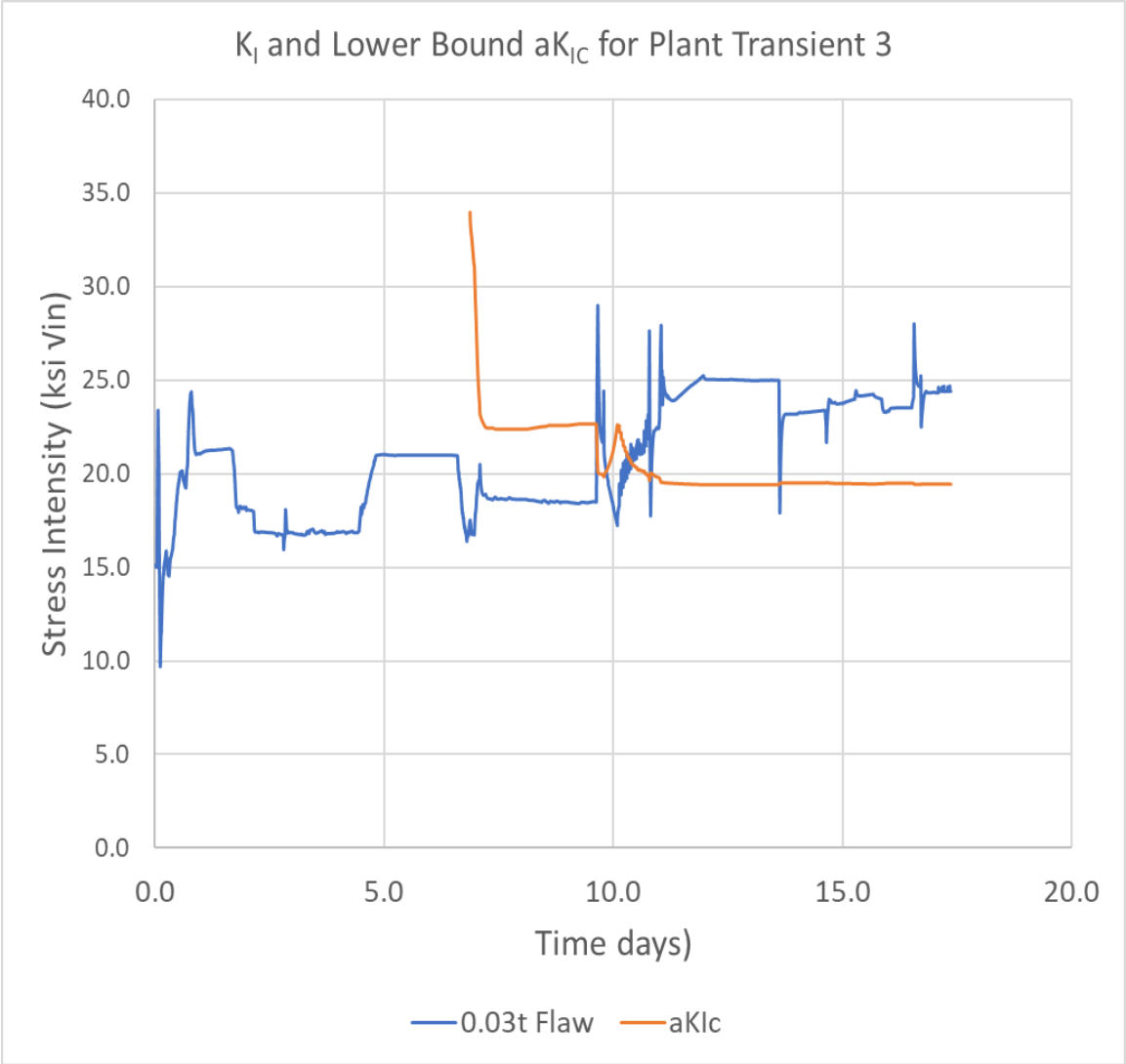

Figure 19: K_I versus Time for Transient 3

Plant Transient 4 involved a cooldown over 60 hours from 540°F to about 100°F as shown in Figure 20. The pressure in Transient 4 decreased from 2.2 ksi to about 0.4 ksi at 15 hours and remained at this pressure until about 50 hours when the pressured was further reduced to atmospheric pressure. Transient 4 is an example of a cooldown that reduces pressure close to the saturation pressure curve in Figure 12.

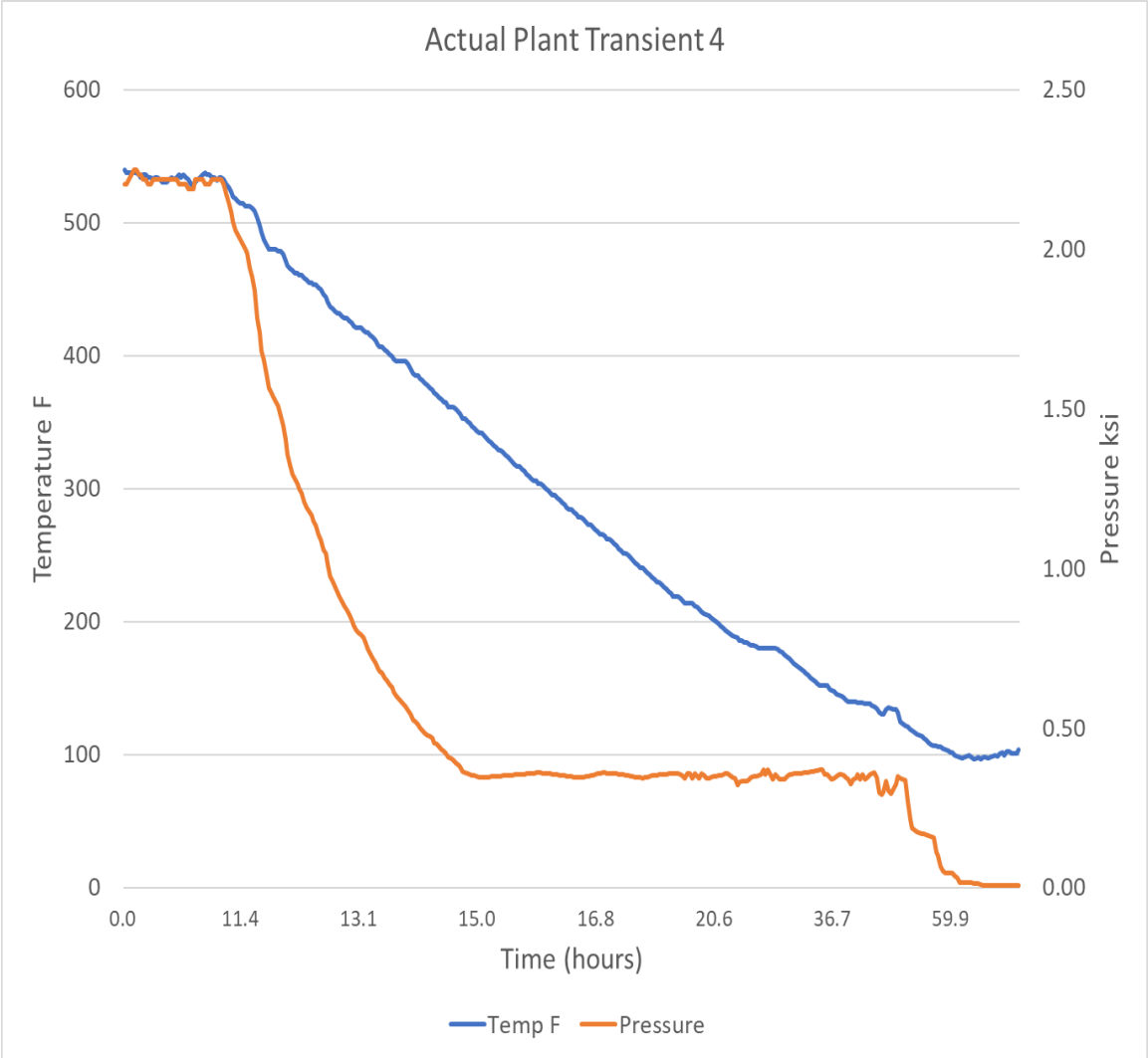

Figure 20: Plant Transient 4 Temperature and Pressure versus Time

Transient 4 was analyzed with FAVOR for 0.03 t flaw and the K_I (Time) for this transient is shown in Figure 21 along with a plot of the lower bound Weibull aK_{IC} curve. The 0.03 t flaw K_I (Time) is relatively flat for the first 40 hours with a peak at about 45 hours near the end of the transient when RCS temperature drops below 100°F. Because this K_I (Time) peak at 45 hours is higher than any previous K_I (Time) and higher than the lower bound of the Weibull curve, there is some probability of crack initiation.

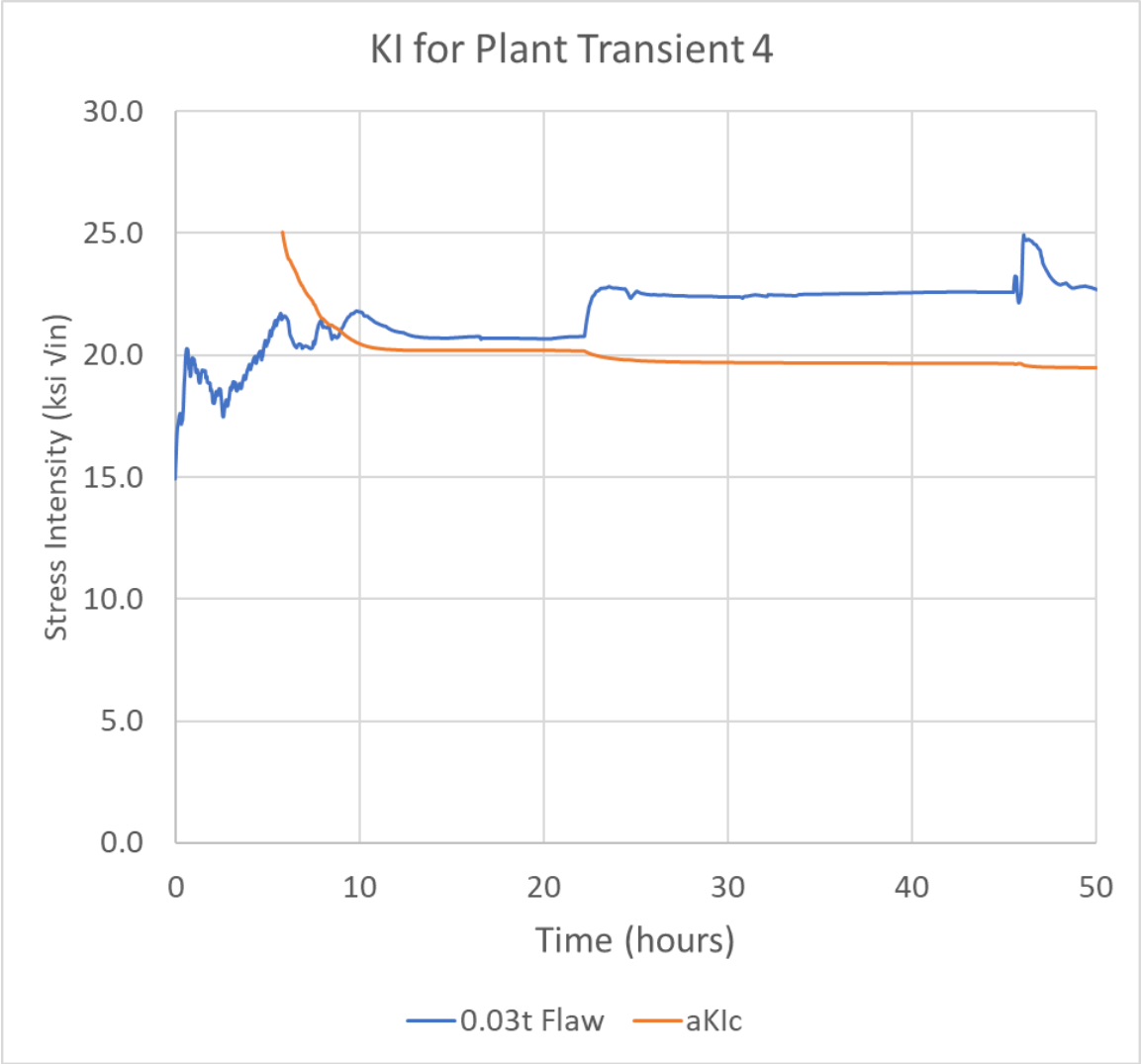

Figure 21: K_I versus time for Transient 4

4.3 Temperature/Pressure Curves for Shallow Flaw Analyses

As discussed in Section 3, maintaining pressure at initial plant operating pressure during cooldown until the maximum pressure determined by ASME Nonmandatory Appendix G to SC-XI (see Figure 12) drops below this initial pressure, results in a peak of K_I (Time) when pressure is first reduced. Because the temperature is relatively high when the pressure is first reduced, this profile may overestimate WPS for some shallow flaws compared with more realistic cooldown profiles.

As shown in Section 3, temperature profiles where both temperature and pressure are reduced together early in the transient and then follow the maximum pressure determined ASME Nonmandatory Appendix G to SC-XI procedures have equal CPI and CPF for the 0.03 t flaws (see Table 8). With reduced pressure, the CPI and CPF for some surface-breaking flaws deeper than 0.03 t may be significantly higher than for the ASME Nonmandatory Appendix G to SC-XI procedure profile. As shown in Table 2, the 0.03 t flaws have higher CPI and CPF than deeper flaws for all cooldown curves evaluated.

The four actual plant transients evaluated in the Section 4.2 show that plant operators routinely reduce pressure and temperature together. As shown in Figures Figure 15, Figure 17, Figure 19, and Figure 21, these actual plant cooldowns produce a K_I (Time) peak for the 0.03 t shallow flaw at about the same time as when the RCS temperature drops below 100°F. Because the 0.03 t flaw peak K_I (Time) for these actual plant cooldowns occurs after the K_I (Time) exceeds the lower bound Weibull curve, there is some probability for crack initiation during these transients.

The reduced pressure 2 curve shown in Figure 12 reduces pressure and temperature together early in the cooldown and then merges into maximum pressure allowed by ASME Nonmandatory Appendix G to SC-XI at lower temperature. Using this reduced pressure 2 P-T profile for analyzing cooldown transients will ensure that WPS is not overestimated and that the K_I for shallow flaws is conservatively calculated at low temperature.

4.4 Shallow CPI and CPF analyses with Reduced Pressure 2 Cooldown, SFT of 563°F and Equation 1 CTE

Based on the sensitivity studies discussed above, the FAVOR calculated CPI and CPF for shallow flaws are sensitive to cooldown P-T profile, SFT and CTE. FAVOR analyses were performed to determine the K_I (Temperature) for a cooldown (constant rate of 100°F/hour) at the reduced pressure 2 profile shown in Figure 12 along with SFT of 563°F and Equation 1 clad CTE. These analyses use the FAVOR Palisades 60 EFPY model developed during the PTS reevaluation.

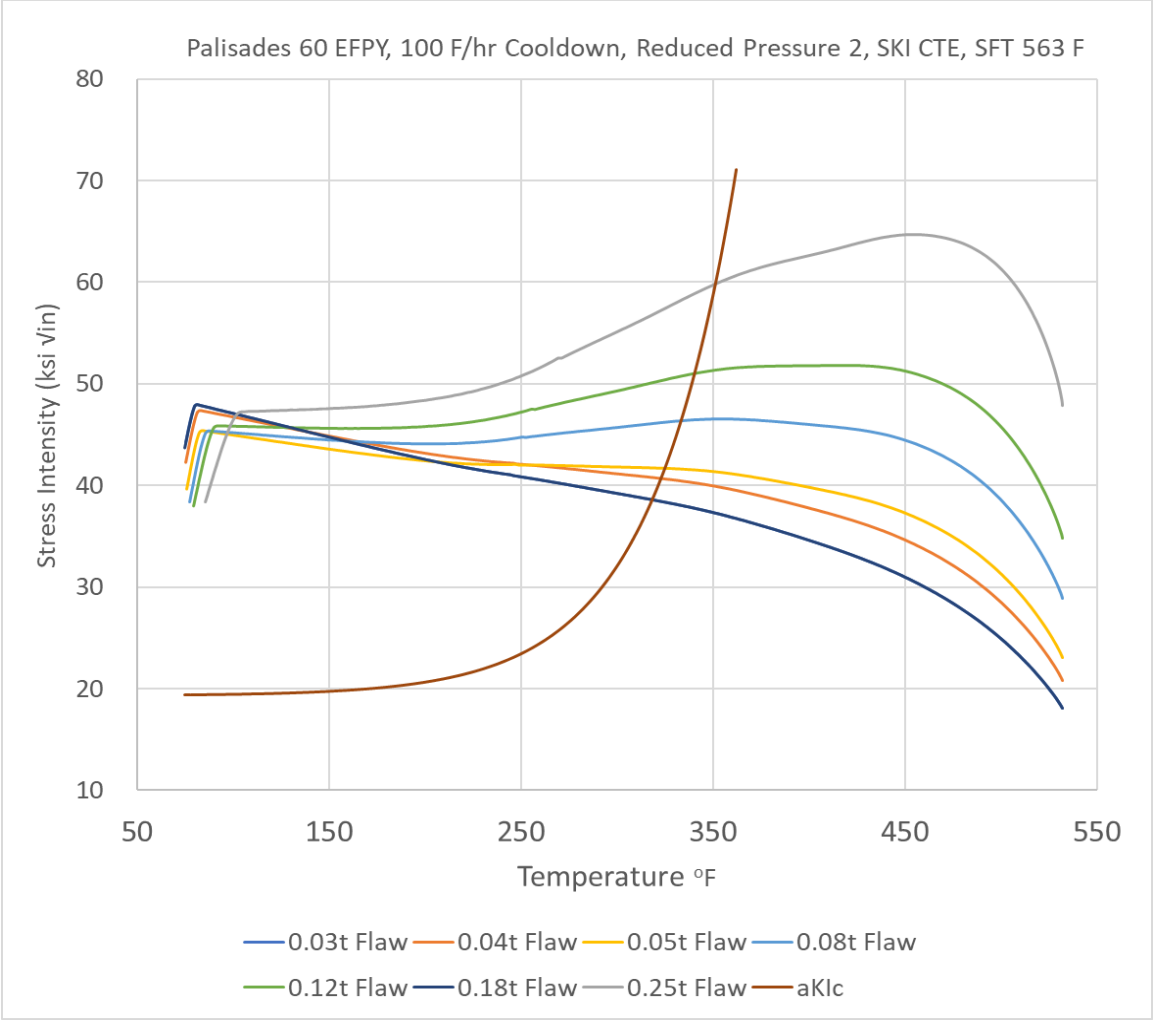

Figure 22: K_I for Palisades 100 F/hour Cooldown, SFT of 563°F and SKI Clad CTE

A plot of the FAVOR deterministic analyses of K_I (Temperature) for 0.03 t to 0.25 t flaw depths is shown in Figure 22. The FAVOR calculated K_I is plotted as a function of temperature to facilitate comparisons of K_I for various flaw depths along with the lower bound Weibull aKIc on a single plot. For flaw depths greater than 0.05 t, the K_I (Temperature) peaks before the K_I(Temperature) crosses the lower bound Weibull aKIc curve during the cooldown.

The maximum K_I and the temperature at which the maximum K_I occurs is shown in Table 9 along with the calculated CPI and CPF for each of these flaw depths. Because the K_I in Figure 22 peaks before the K_I crosses the lower Weibull distribution curve for flaw depths greater than 0.05 t, these deeper flaws are protected from crack initiation by WPS. The relatively high CPI and CPF for flaw depths of 0.03 t to 0.05 t are caused by having K_I peak at low temperature as shown in Table 9 after crossing the lower bound Weibull aKIc curve.

Table 9: CPI and CPF for Palisades 100°F/hour Cooldown, SFT of 563°F and SKI Clad CTE versus Flaw Depth

CPI and CPF for 'reduce pressure 2' transient (Figure 12), 100°F/hour, SFT 563°F, SKI CTE				
Flaw Depth	Maximum K_I (ksiVin)	Temperature at maximum K_I (°F)	CPI_{mean}	CPF_{mean}
0.03 t	47.9	81	**1.70E-02**	**7.77E-03**
0.04 t	47.4	83	**9.62E-03**	**4.11E-03**
0.05 t	45.4	84	**4.56E-03**	**2.13E-03**
0.08 t	46.6	356	2.80E-09	0.00E+00
0.12 t	51.8	422	0.00E+00	0.00E+00
0.18 t	58.6	436	0.00E+00	0.00E+00
0.25 t	64.7	457	0.00E+00	0.00E+00

Note: bold value represent CPF higher than 1E-06, which was the threshold for further investigation

The analyses shown in Figure 22 and Table 9 combine conservative assumptions for cooldown rate and P/T profile, SFT and CTE. More realistic assumptions would result in lower mean CPI and CPF values. However, as shown in Section 4.2, actual plant cooldown temperature/pressure profiles, with less conservative values of SFT and CTE, indicate that shallow flaws may exhibit peak K_I (Time) profiles that peak at low temperature and that exceed the lower bound Weibull aKIc curve. Because these actual transients tend to take place over extended time periods, it is difficult to quantify the converged mean CPI and CPF for these actual transients. As discussed in Section 0, additional FAVOR PFM shallow flaw analyses are recommended to evaluate shallow flaw CPI and CPF based on realistic plant cooldown transients.

5 Shop Hydro and Previous Transient Shallow Flaw Pre-Stress

The shallow flaw analyses in the previous sections of this report use FAVOR analyses that consider WPS only from the individual specific transient being evaluated. WPS produces changes in the flaw tip that prevent brittle fracture at future time. One potential transient that would pre-stress manufacturing related flaws, is the initial shop hydrostatic test. Vessel pressure testing requirements are addressed in UG-99 and UG-100 in ASME Code Section VIII Div. 1. Reference (8) provides shop hydro minimum test temperature set by the pressure vessel minimum design metal temperature, as stated in the pressure vessel design document, and a maximum test temperature of 120 ˚F.

The maximum hydrostatic test temperature of 120 °F results in lower thermal and total pre-stress than a lower test temperature. FAVOR calculated K_I versus pressure (from the initial 0.0 ksi to the maximum 3.125 ksi test pressure) are shown in Figure 23. These analyses used the Palisades reactor vessel geometry and an assumed test temperature of 120°F. Results are provided for various surface breaking flaw depths from 0.03 t to 0.25 t.

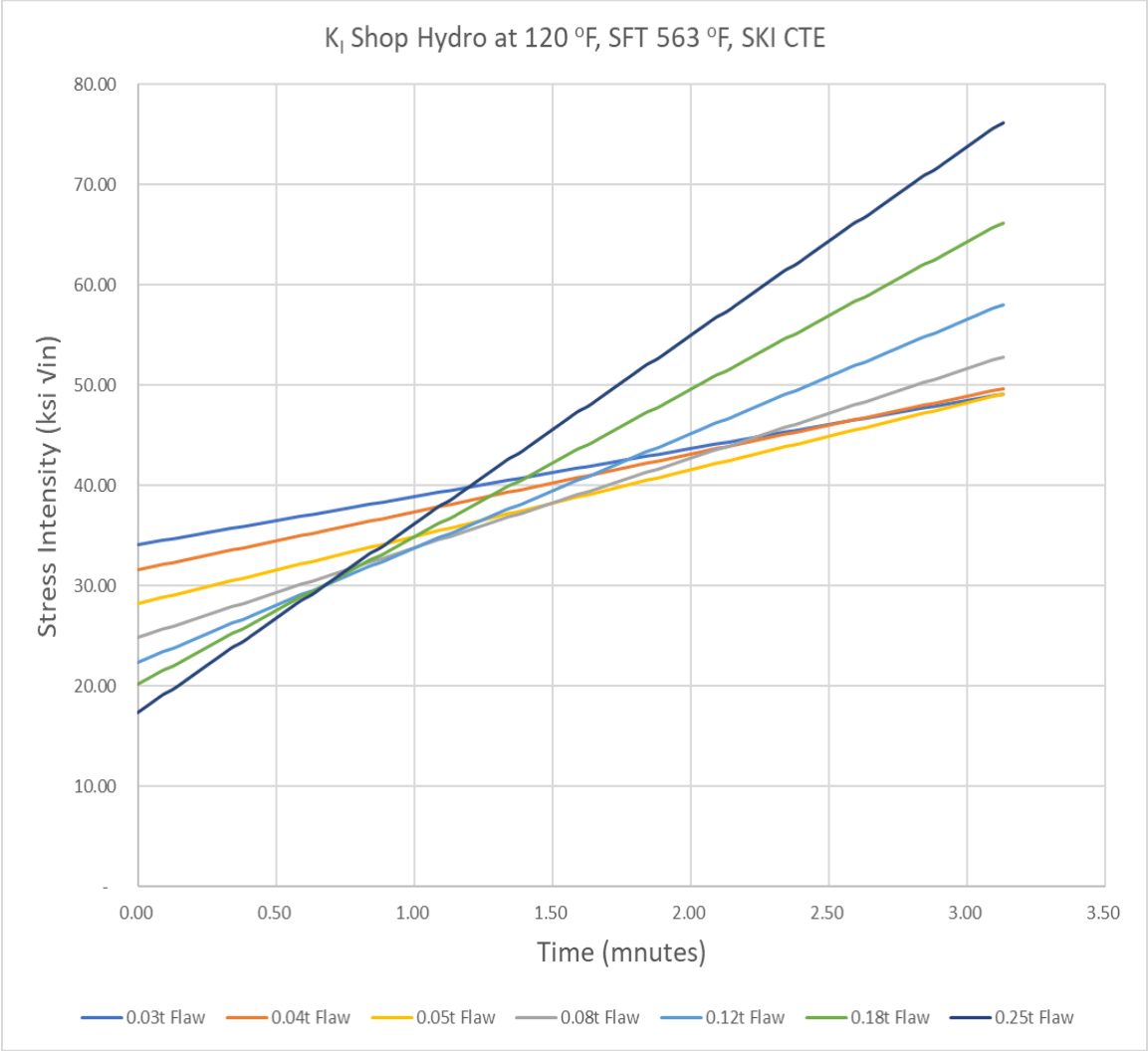

Figure 23: K_I Versus Pressure for Palisades Shop Hydro

Table 10 provides a comparison of the maximum K_I versus flaw depth for the cooldown transient analyses shown in Table 9 with the shop hydro K_I. As shown in Table 10, the shop hydro K_I is greater than the cooldown K_I for all flaw depths. WPS during a single transient is an accepted assumption for PFM analyses. However, WPS from a shop hydro that may have occurred more than 50 years before the cooldown transient has not been previously credited for PFM analyses.

In the cases evaluated in Table 10, the maximum shop hydro stress exceeds the maximum stress from the plant cooldown evaluated in Section 4.4 Changes in SFT and clad CTE have approximately equal impact on both the shop hydro and cooldown calculated K_I. Therefore, changes in these values would not significantly change the margin between shop hydro and cooldown transient K_I values shown in Table 10. However, the lower plant transient cooldown rate and pressure shown for actual transients in Section 4.2would reduce the cooldown transient maximum K_I and provide additional margin.

If pre-service flaws extend deeper during RPV service, shop hydro WPS may not be effective in preventing shallow flaw crack initiation later in plant life. Reference (9) states that "Fatigue crack growth is recognized as the primary degradation mechanism in the carbon and low alloy steel components in PWR Nuclear Steam Supply System (NSSS), that could contribute to any potential growth of existing flaws in the component base materials and weld metals." In Reference (10), the PWR Owners group provided responses to NRC requests for additional information on Revision 1 of Reference (9), including Figure A-4300-2, Reference Fatigue Crack Growth Curves for Carbon and Low Alloy Ferritic Steels Exposed to Water Environments. This figure shows crack growth rates of approximately 10^{-5} to 10^{-3} inches per fatigue cycle depending on the applied stress. At the higher growth rate of 0.001 inches per fatigue cycle, an initial 0.03 t flaw (0.263 inches) would increase to a depth of 0.363 inches in 100 fatigue cycles. It is beyond the scope of this scoping study to determine whether crack growth rate would impact shop hydro WPS and further reviews of fatigue crack growth would be needed to determine how long shop hydro is effective in preventing crack initiation.

Table 10: Comparison of Palisades Cooldown and Shop Hydro Maximum K_I

Evaluation of Shop Hydro at Test Temperature of 120 °F and pareesure of 3.125 ksi				
	Flaw Depth	**Maximum K_I ksi √in**	**Shop Hydro K_I ksi √in**	***% of Shop Hydro***
Palisades SFT 563 RP2 Cooldown at 100 F/hr, SKI CTE	0.03t	47.9	49.12	98%
Palisades SFT 563 RP2 Cooldown at 100 F/hr, SKI CTE	0.04t	47.4	49.68	95%
Palisades SFT 563 RP2 Cooldown at 100 F/hr, SKI CTE	0.05t	45.4	49.10	93%
Palisades SFT 563 RP2 Cooldown at 100 F/hr, SKI CTE	0.08t	46.6	52.79	88%
Palisades SFT 563 RP2 Cooldown at 100 F/hr, SKI CTE	0.12t	51.8	58.00	89%
Palisades SFT 563 RP2 Cooldown at 100 F/hr, SKI CTE	0.18t	58.6	66.17	89%
Palisades SFT 563 RP2 Cooldown at 100 F/hr, SKI CTE	0.25t	64.7	76.15	85%

6 Summary and Recommended Additional Analyses

FAVOR analyses of shallow internal surface-breaking flaws indicate that there may be a relatively high Conditional Probability of crack Initiation (CPI) for these flaws. Because plant cooldown transients are normal plant operations that occur with a frequency of at least once per refueling cycle, additional FAVOR PFM analyses should be performed to determine whether normal plant cooldown transients should be considered in RPV structural integrity evaluations.

The frequency and depth of inside surface breaking flaws shown in Reference (3) is based on limited data and the flaw probability may be conservative when compared with the actual frequency of inside surface-breaking flaws. Reference (3) states that surface-breaking flaws are not expected to exceed one weld bead in depth and that no flaws are expected to extend through multi-layer stainless steel clad into the vessel base metal. The analyses in Reference (9) assumes for conservatism that all PWR vessels have single layer clad. However, only one of the four PWR pilot plant vessels shown in Reference (9) has single layer clad.

Use of a WPS brittle failure model is accepted as a standard part of FAVOR PFM analyses. The FAVOR PFM model requires that the following two conditions be true for there to be a possibility of crack initiation:

(1) the applied value of K_I should exceed the minimum value of K_I resistance as defined by the lower bound Weibull aKIc curve, and

(2) the applied value of K_I should both be increasing with time and exceed all previous maximums during the loading event being considered.

Previous FAVOR analyses have only considered the single transient being evaluated to apply these two criteria. As discussed in section 5it may be possible to show that previous plant cooldown transients, including the pre-service shop hydro, provide WPS to eliminate crack initiation based on criteria two above. However, any analysis using WPS from shop hydro and previous transients should evaluate whether fatigue crack growth limits the time that past WPS is effective in preventing crack initiation.

As shown in the Section 3 cooldown at system operating pressure until the maximum pressure determined by according to ASME Nonmandatory Appendix G to SC-X drops below this operating pressure, may overestimate the potential for WPS. The evaluation of the four actual plant transients in Section 4.2 shows that the 0.03 t flaw K_I (Time) peaks at low temperature. Using the P-T profile identified as reduced pressure 2 in Figure 12 will ensure that WPS is not overestimated.

Previous shallow flaw evaluations suggested that lower CRS may justify a lower SFT. However, a literature review identified higher CRS measurements than the values used in ORNL 2016 to support an SFT of 488°F. CRS measurements published by the Swedish Nuclear Power Inspectorate (SKI) in Reference (6) and the evaluations of SFT in this report do not support a reduction in SFT below 488°F. As discussed in Sections 3 and 3.2, the SFT of 488°F used in ORNL 2016 may not bound SFT for all reactor vessels. A sensitivity for SFT values higher and lower than 488°F is shown in Table 4. Based the analyses shown in Table 4, CPI and CPF are sensitive to SFT. Therefore, additional studies are recommended to quantify CRS from measured values to ensure that an appropriate SFT is used in FAVOR.

During the literature review for SFT and CRS, additional values of stainless-steel clad CTE higher than those used in the ORNL 2016 FAVOR analyses were identified in References (6) and (7). As discussed in Section 3.3, the clad CTE values from the different references between 3% and 10% higher than the higher CTE used in ORNL 2016. As shown in Table 7, FAVOR calculated CPI and CPF are sensitive to these relatively small changes in clad CTE.

The combined impact (1) cooldown with the reduced pressure 2 profile, (2) increased SFT from 488°F to 563°F, and (3) use of the (Reference (6)) stainless-steel clad CTE is evaluated in Section 4.4 and presented in Table 9. This combined case results in significantly higher CPI and CPF values than the results presented in ORNL 2016.

Because the scoping and sensitivity studies in this report did not identify a basis for a significant reduction of the FAVOR calculated mean CPI and CPF in ORNL 2016, additional shallow flaw analyses based on the complete vessel loading history including shop hydro should be evaluated to determine whether WPS from prior transients significantly reduces FAVOR calculated CPI and CPF.

This shallow flaw scooping study shows that the potential for brittle fracture from shallow flaws may be greater than the CPI and CPF values shown in ORNL 2016. The following additional analyses are recommended to further evaluate further whether shallow surface-breaking flaws significantly increase probability of RPV crack initiation and the Through Wall Crack Frequency (TWCF):

(1) Perform literature reviews and additional analyses to determine whether pre-stress during shop hydro can be better quantified and whether this pre-stress can be relied on to prevent brittle fracture during normal plant cooldown transients. This analysis should include an evaluation of whether fatigue crack growth of surface-breaking flaws limits the time that shop hydro and other plant transient WPS will be effective in preventing crack initiation.

(2) Perform additional analyses and evaluations of normal plant cooldown transients. Cooldown to 70°F at a constant high cooldown rate of 100°F/hour produces relatively high applied K_I values compared with slower cooldown rates as the plant temperature approaches 70°F. Cooldown rate limits from typical plant cooldown practice and the design of plant residual heat removal systems should be evaluated.

(3) Because the current FAVOR WPS model only evaluates applied K_I during individual transients, an option should be added to the FAVOR that allows the user to input historical applied K_I values from shop hydro or other sources for WPS evaluations.

(4) Additional evaluations of shallow flaw probability versus depth should be performed including an evaluation of whether clad defects extending into the base metal are prevented by two-layer cladding.

(5) Improvements to the FAVOR code to allow evaluation of as-found flaws should be considered.

(6) RPV 10-year In-Service Inspection reports should be reviewed to determine whether shallow surface breaking flaws have been identified during these inspections.

After additional discussion and development of a shallow flaw analysis matrix, prototypical and actual plant cooldown transients for PWRs and BWRs should be evaluated to assess the effect of shallow flaws on the integrity of the vessel.

7 References

1. **Bass, Richard B, et al.** *The Effect of Shallow Inside-Surface-Breaking Flaws on the Probability of Brittle Fracture of Reactors Subjected to Postulated and Actual Operational Cool- Down Transients: A Status Report.* s.l. : ORNL/TM-2015/59531/Rev-01, 2016.
2. *A Computer Code for Fracture Mechanics Analysis of Nuclear Reactor Pressure Vessels, PVP 2017-65262.* **Bass, Richard B, et al.** Waikoloa, Hawaii : Procedings of the ASME 2017 Pressure Vessels and Piping Conference, July 16-20, 2017.
3. **F. A. Simonen, S. R. Doctor, G. J. Schuster, and P. G. Heasler.** *PNNL-14268, Rev. 1, A Generalized Procedure for Generating Flaw-Related Inputs for the FAVOR Code.* s.l. : Pacific Northwest National Laboratory, October 2003.
4. **ASME.** *ASME Boiler and Pressure Vessel Code, Section XI, Appendix G.* New York : s.n., 2004.
5. **Williams, P.T., et al.** *Fracture Analysis of Vessels – Oak Ridge FAVOR, v16.1, Computer Code: Theory and Implementation of Algorithms, Methods, and Correlations, ORNL/LTR-2016/309.* s.l. : Oak Ridge National Laboratory, Spetember 2016.
6. **Iradj, Sattari-Far and Andersson, Magnus.** *Cladding Effects on Structural Integrity of Nuclear Components.* s.l. : Swedish Nucler Power Inspectorate (SKI), June 2006.
7. **Atlas Steels.** *Stainless Steel Datasheets.* s.l. : Atlas Steels Technical Department, August 2013.
8. **Inspection-for-Industry.com.** Vessel Pressure Testing. *https://www.inspection-for-industry.com/.* [Online]
9. **Bruce A. Bishop, Chryl L, Boggess, Nathan A. Palm.** *WCAP-16168-NP-A Rev 3, Risk-INfromed Extension of the Reactor Vessel In-Service Inspection Interval.* October 2011.
10. **PWR Owners Group.** *Responses to Request for Infromation on WCAP-16168-NP, Rev 1.* October 2007.